

University of Babylon
Faculty of Engineering
Department of Biomedical Engineering



Wireless Powering of Biosensors

A Project Submitted in Partial Fulfillment of the Requirements for the Degree of
Bachelor of Science (B.Sc.) in Biomedical Engineering.

By

Fatima Nagi Abd

Amani Ali Abd

Supervisors

Prof. Dr. Abdulkareem Mokif Obais

Academic year 2021/2022

جامعة بابل / كلية الهندسة

قسم هندسة الطب الحيوي



الطاقة اللاسلكية لأجهزة الاستشعار الحيوية

قدم هذا المشروع لإستكمال جزء من متطلبات الحصول على
درجة البكالوريوس في هندسة الطب الحيوي

قدم من قبل:

فاطمة ناجي عبد

اماني علي عبد

إشراف

الدكتور عبد الكريم مخيف

العام الدراسي 2021/2022

Copyright © 2022. All rights reserved, no part of this project may be reproduced in any form, electronic or mechanical, including photocopy, recording, scanning, or any information, without the permission in writing from the author or the department of Biomedical Engineering, university of Babylon.



الاهداء

في هذه اللحظة عانيت كثيرا وواجهت الكثير من الصعوبات والعقبات ، ومع كل هذا قررت أن أتغلب على هذه الصعوبات بإيمان راسخ بالله العظيم.

لأمي وابي وأختي وجميع أصدقائي ، لن أنسى أساتذتي ، لقد قدموا لي النصيحة ، وهم لا يبخلون بمعرفتهم ووقتهم.

هذه أطروحة التخرج ، كهدية خاصة لكم ، لأعبر لكم عن أعمق احترامي وامتناني.

Certificate

The project entitled:

Wireless Powering of Biosensors

Which is being submitted by

Fatima Nagi Abd

Amani AliAbd

In the fulfillment of requirement for the award of the B.Sc. degree in Biomedical Engineering. This has been carried out under my supervision and accepted for presentation & examination.

Signature :

Supervisor's name :

Date: /...../2022

The Supervisor...

Table of Contents:

Subject	Page No.
Contents	I
المستخلص	IV
Absract	V
CHAPTER ONE INTRODUCTION	
1.1 General Overview	1
1.2 Problem Statement	2
1.3 Objectives	2
1.4 Literature Review	3
CHAPTER TWO WIRELESS POWERING OF BIOSENSORS	
2.1 Introduction	13
2.2 Different Approaches for Wireless Power Transfer Systems	14
2.3 Principles of WPT Systems	17
2.4 Mat-Based Wireless Power Transfer to Moving Targets	19
2.5 The Categories of Wireless Power Transfer	20
2.5.1 Near Field Wireless Power Transmission	22
2.5.2 Far Field Wireless Power Transmission	27

2.5.3 Mid Field Wireless Power Transmission	27
2.6 Resonant Coupling Wireless Power Transfer Structures	27
2.6.1 Two-Coil Based Wireless Power Transfer Structure	27
2.6.2 Three-Coil Based Wireless Power Transfer Structure	28
2.6.3 Four-Coil Based Wireless Power Transfer Structure	29
2.7 Implantable Biomedical Devices for POC Diagnostics	29
2.8 General Wireless Power Transmission (WPT) system	32
CHAPTER THREE THE PROPOSED WPT SYSTEMS	
3.1. Introduction	36
3.2. Design of Planar Spiral Coils	36
3.3. The Inductive Link	38
3.4. Proposed WPT System for Skin Implantable Biosensors	42
3.5. The Proposed WPT System for deep Implantable Biosensors	44
CHAPTER FOUR RESULTS AND DISCUSSION	
4.1. Introduction	47
4.2. Results of Powering Skin Implantable Biosensors	47
4.3. Results of Powering Deeply embedded Biosensors	51
CHAPTER FIVE CONCLUSION AND FUTURE WORK	
5.1. Conclusion	54
5.2. Future Work	54

References	55
------------	----

المخلص

يتم تضمين كل من نقل الطاقة اللاسلكية أو نقل الطاقة الكهرومغناطيسية في نقل الطاقة الكهربائية بدون أسلاك ، ولكن كروابط مادية. في نظام نقل الطاقة اللاسلكية ، يولد جهاز الإرسال ، الذي يتم تشغيله بواسطة الطاقة الكهربائية من مصدر طاقة ، مجالاً كهرومغناطيسياً متغيراً بمرور الوقت ، والذي ينقل الطاقة عبر الفضاء إلى جهاز استقبال ، والذي يستخرج الطاقة من الحقل ويوزدها بالكهرباء حمل. يمكن لتقنية نقل الطاقة اللاسلكية أن تلغي استخدام الأسلاك والبطاريات ، وبالتالي زيادة التنقل والراحة والسلامة للأجهزة الإلكترونية لجميع المستخدمين. يعد نقل الطاقة اللاسلكي مفيداً لتشغيل الأجهزة الكهربائية حيث تكون الأسلاك المتصلة غير ملائمة أو خطيرة أو غير ممكنة.

في هذا العمل ، يتم استغلال نقل الطاقة اللاسلكية لنقل الطاقة إلى أجهزة الاستشعار الحيوية المزروعة في جسم الإنسان. تم اقتراح نظامين للطاقة لهذا الغرض. يتعلق النظام الأول بتشغيل أجهزة الاستشعار الحيوية المزروعة على السطح ، بينما يتعامل النظام الثاني مع تشغيل أجهزة الاستشعار الحيوية المتأصلة بعمق في جسم الإنسان. يتم أيضاً تضمين شحن البطاريات المدمجة في هذا العمل.

ABSTRACT

Wireless power transfer (WPT), wireless power transmission, wireless energy transmission (WET), or electromagnetic power transfer are all incorporated in the transmission of electrical energy without wires, but as physical links. In a wireless power transmission system, a transmitter device, driven by electric power from a power source, generates a time-varying electromagnetic field, which transmits power across space to a receiver device, which extracts power from the field and supplies it to an electrical load. The technology of wireless power transmission can eliminate the use of the wires and batteries, thus increasing the mobility, convenience, and safety of an electronic device for all users. Wireless power transfer is useful to power electrical devices where interconnecting wires are inconvenient, hazardous, or are not possible.

In this work, the wireless power transfer is exploited for transferring power to implanted biosensors in human body. Two powering system are proposed for this purpose. The first system concerns powering surface implanted biosensors, whereas the second deals with powering deeply embedded biosensors in human body. Charging of embedded batteries is also incorporated in this work.

CHAPTER ONE

INTRODUCTION

1.1 General Overview

Biosensors are considered as a fast-growing field, as they have been shown to be very helpful in our daily life, playing roles in industries such as agriculture, food safety, homeland security, bioprocessing, environmental monitoring, and industrial monitoring. Beyond these, the application of biosensing in medicine and biomedical engineering may have the highest potential for growth and for affecting human quality of life in the near future. This potential is driven by the need for new and improved devices and technologies with improved sensitivity, specificity, reliability, and biocompatibility, which can solve and manage medical and health problems such as heart diseases, cancer, or diabetes, among others. For example, since tumors present a unique microenvironment, an implantable biosensor near a tumor would allow precise monitoring of the disease's progression. The first biosensor reported for use in vivo was based on magnetic nanoparticles and was used to detect soluble cancer biomarkers in mice. Since then, the research field of implantable biosensors has become a hot topic in the scientific community [1].

In recent years, medical progress has evolved with an increased interest in instruments for sensing and controlling the specific functions of the brain. These medical instruments considerably decrease morbidity and improve the standard of life for certain patients. Sensor systems are now quite advanced but providing power to these devices is still a major challenge. Wireless power transmission (WPT) is a critical technology that provides a secure alternative mechanism for wireless power and communication with implantable medical devices. WPT approaches for implantable medical devices have been utilized based on applications. For instance, the inductive coupling tactic is mostly employed for transmission of energy to neuro-stimulators, and the ultrasonic method is used for deep-seated implants. This article provides a study concentrating on popular WPT techniques for implantable medical devices (IMDs) including inductive coupling, microwave, ultrasound, and hybrid WPT systems consisting of two approaches

combined. Moreover, an overview of the major works is analyzed with a comparison of their major design elements, operating frequency, distance, efficiency, and harvested power [2].

A sensor is a device that receives a signal or stimulus and responds to the stimulus in the form of an electrical signal. The output signals correspond to some forms of electrical signal, such as current or voltage. The sensor is a device that receives different kinds of signal i.e. physical, chemical or biological signal and converts them into an electric signal. The sensors are classified into different types based on the applications, input signal, and conversion mechanism, material used in sensor characteristics such as cost, accuracy or range [3].

1.2 Problem Statement

A wireless power transfer technique is used to solve the problem of avoiding surgical process during replacing the battery of the implanted sensor or charging it. The solutions are introduced to power the implanted sensors at distances ranging from 1cm to 30cm.

1.3 Objectives

Two proposed systems are introduced here; wireless power transfer by direct coupling method for very close distances between external circuits and the implanted sensors and the wireless power transfer by loosely coupled method for distances ranging between 1cm and 30cm.

The objectives of this work for both proposed system are directed to

- 1- Design an RF power amplifier in class-E topology.
- 2- Choose and design the best conductor coil type suitable for the transmitter and receiver.
- 3- Design a rectifier circuit for detecting the modulated signal.
- 4- Design a stabilizing circuit for regulating the voltage needed for powering the implanted sensors.

1.4 Literature Review

Since wireless power transfer technology (WPT) gains its popularity, broad range of application and research are performed in the field of medical implantable applications. In this paper, we review the technical status of WPT system applied to medical implant devices. As a practical application of this technology, the current achievements and challenges of wireless capsule endoscopy are reviewed and analyzed, in view of its design, functional requirement and related issues in WPT. And WPT application to artificial heart is also discussed. Based upon the analysis, we propose a research directions and WPT consideration in designing a WPT system for implantable medical applications [4].

In [5], the recent progress in the field of point of care diagnostic (POCD) devices were described. The main challenge in developing wireless integrated biosensors is the development of integrated sensors and circuits on the same chip. We also put forward the advanced CMOS techniques used to develop electrochemical sensors. Among these, electrochemical impedometric, amperometric, voltometric and ISFET methods were comprehensively described, with further details of interface circuits and non-idealities, which can be compensated mostly using specific circuitries. The road map of point-of-care diagnostic technologies is the development of RF integrated sensors and actuators functionalized with recognition element for specific sensing purposes and CMOS will play a very critical role to microchip scale integration technology in future development in this field.

Energy harvesting is identified as a promising alternative solution for powering implantable biosensors. It can completely replace the batteries, which are introducing many limitations, and it enables the development of self-powered implantable biosensors. An interface circuit is necessary to correct for differences in the voltage and power levels provided by an energy harvesting device from one side, and required by biosensor circuits from another. This thesis investigates the available energy harvesting sources within the human body, selects the most suitable one and proposes the power management unit (PMU), which serves as an interface between a harvester and biosensor

circuits. The PMU targets the efficient power transfer from the selected source to the implantable biosensor circuits [6].

Wireless power Transfer (WPT) technique, based on inductive links, has been admitted as a promising solution for powering biomedical implants. Ensuring a stable power delivery via inductive links in implants under all conditions, however, has been a challenging design problem. One of the issues that negatively impacts the performance of wireless power transfer (WPT) links in implants, is the misalignment in the position of the transmitter and receiver coils, which could naturally occur as a result of body movement or changes in the biological environment [7].

A system for wireless power transfer and data communication of implantable bio-monitoring systems is presented. The proposed solution uses a servo-controlled power transmitter moved under the animal moving space. An x- y movable magnetic coil transmits the required power with a level able to keep constant received energy by the bio-sensor system. The power is transferred via the optimized remote powering link at 13.56 MHz. The received ac signal is converted to dc voltage with a passive full-wave integrated rectifier and the voltage regulator supplies 1.8 V for the implantable sensor system. The sensor control and readout circuit measures the current on the bio-sensors and transmit the data to the transmitter. The sensor data are transmitted to an external reader by a low-power OOK transmitter and received by a custom designed receiver at 869 MHz. The results are shown in a tablet computer in real time continuously. The long-term characterization of the implantable system is verified by a fully bio-compatible packaged implant with 30 days measurement. A complete prototype is also presented to prove the overall system performance with the experimental in vitro measurement [8].

Successful physiological integration of electronics will open the doors to new methods of treatment and diagnoses. One of the key challenges of this integration is designing devices as small as possible while still maintaining high functionality, such as bio-signal recording, processing, telemetry, and stimulation. Wireless power transfer (WPT) can help shrink a device's footprint by removing the need for bulky batteries. While many modalities of WPT exist for biomedical applications, the optimal power transfer efficiency (PTE) is seldom achieved due to improper impedance matching [9].

CHAPTER ONE INTRODUCTION

Wireless power transfer (WPT) systems have become increasingly suitable solutions for the electrical powering of advanced multifunctional micro-electronic devices such as those found in current biomedical implants. The design and implementation of high power transfer efficiency WPT systems are, however, challenging. The size of the WPT system, the separation distance between the outside environment and location of the implanted medical device inside the body, the operating frequency and tissue safety due to power dissipation are key parameters to consider in the design of WPT systems. This article provides a systematic review of the wide range of WPT systems that have been investigated over the last two decades to improve overall system performance. The various strategies implemented to transfer wireless power in implantable medical devices (IMDs) were reviewed, which includes capacitive coupling, inductive coupling, magnetic resonance coupling and, more recently, acoustic and optical powering methods [10].

Wireless power transfer (WPT) working at megahertz (MHz) is widely considered a promising technology for the mid-range transfer of low power. In the biomedical implantable WPT systems, the receiving coil is small. Meanwhile, in real applications, the required transfer distance is large. Thus, the coupling coefficient k is low. For the applications of large load, the low coupling coefficient k and large load RL deteriorate the system efficiency largely. This paper proposes an optimal design method of MHz WPT systems for biomedical implants. A capacitive L-matching network is inserted in the conventional MHz Class E² WPT system to enlarge the reflected impedance of the receiving coil on the transmitting side, i.e., improve the power transfer capability and efficiency of the coupling coils. Then the input impedance of the matching network and efficiency of the proposed MHz WPT system are derived and serve as the basis of the proposed parameter design procedure. Based on the circuit improvement and analytical derivations, a numerical optimization design method is proposed to optimize the design parameters of the MHz WPT system. The final experiment verifies the feasibility of the design procedure. With loosely coupled coils (coupling coefficient $k=0.035$, distance of the coupling coils=1.5 cm, diameter of receiving coil=1.5 cm), the system efficiency can achieve 36.43% under a 0.5 W power transfer [11].

CHAPTER ONE INTRODUCTION

Conventional resonant inductive coupling wireless power transfer (WPT) systems encounter performance degradation while energizing biomedical implants. This degradation results from the dielectric and conductive characteristics of the tissue, which cause increased radiation and conduction losses, respectively. Moreover, the proximity of a resonator to the high permittivity tissue causes a change in its operating frequency if misalignment occurs. In this report, we propose a metamaterial inspired geometry with near-zero permeability property to overcome these mentioned problems. This metamaterial inspired geometry is stacked split ring resonator metamaterial fed by a driving inductive loop and acts as a WPT transmitter for an in-tissue implanted WPT receiver. The presented demonstrations have confirmed that the proposed metamaterial inspired WPT system outperforms the conventional one. Also, the resonance frequency of the proposed metamaterial inspired TX is negligibly affected by the tissue characteristics, which is of great interest from the design and operation prospects. Furthermore, the proposed WPT system can be used with more than twice the input power of the conventional one while complying with the safety regulations of electromagnetic waves exposure [12].

Commercially available metal inks are mainly designed for planar substrates (for example, polyethylene terephthalate foils or ceramics), and they contain hydrophobic polymer binders that fill the pores in fabrics when printed, thus resulting in hydrophobic electrodes. Here, a low-cost binder-free method for the metallization of woven and nonwoven fabrics is presented that preserves the 3D structure and hydrophilicity of the substrate. Metals such as Au, Ag, and Pt are grown autocatalytically, using metal salts, inside the fibrous network of fabrics at room temperature in a two-step process, with a water-based silicon particle ink acting as precursor. Using this method, (patterned) metallized fabrics are being enabled to be produced with low electrical resistance (less than $3.5 \Omega \text{ sq}^{-1}$). In addition to fabrics, the method is also compatible with other 3D hydrophilic substrates such as nitrocellulose membranes [13].

A technique of wireless power transfer(WPT) system for biomedical applications with backscattering communication a rectifier use with active bias mechanism (dependent and independent stages) overcome the diode device losses has been presented in this paper. A part from conventional and static V_{th} cancellation technique rectifiers, it

CHAPTER ONE INTRODUCTION

achieve more than double efficiency and achieves powerless reduction in both forward and reverse biased conditions, it decrease turn on voltage in forward bias condition along with decrease in reverse leakage current during reverse bias condition. Under the input conditions ($V_{in}=1V_{p-p}$ coupling coefficient's=0.01 at 200MHz frequency with transmitter and receiver inductance of 22nH, actively biased differential drive rectifier able to achieve DC voltage of 880mv for 50k Ω load resistance independent stage and achieves DC voltages of 803.2mv for 50k Ω load resistance in independent stage. Backscattering communication has been performed using switch by changing the resonance frequency of the receiver [14].

Wireless biomedical devices have attracted the attention of researchers over the last decade for health monitoring, syndrome detection, disease prevention, drug delivery and prosthetic limb applications. However, the power requirement is the major constraint for the implementation of such devices. Packaged batteries are the traditional power source for these devices. This source of power is limited by the size and the life time which are the significant parameters for biomedical implants. In addition, any leakage from the battery can cause serious health hazard. Similarly, the transdermal or percutaneous wiring is inconvenient due to bulky size and risk of infection [15].

Miniature implantable electronic devices play increasing roles in modern medicine. In order to implement these devices successfully, the wireless power transfer (WPT) technology is often utilized because it provides an alternative to the battery as the energy source; reduces the size of implant substantially; allows the implant to be placed in a restricted space within the body; reduces both medical cost and chances of complications; and eliminates repeated surgeries for battery replacements. In this work, we present our recent studies on WPT for miniature implants. First, a new implantable coil with a double helix winding is developed which adapts to tubularly shaped organs within the human body, such as blood vessels and nerves. This coil can be made in the planar form and then wrapped around the tubular organ, greatly simplifying the surgical procedure for device implantation. Second, in order to support a variety of experiments (e.g., drug evaluation) using a rodent animal model, we present a special WPT transceiver system with a relatively large power transmitter and a miniature implantable

power receiver. We present a multi-coil design that allows steady power transfer from the floor of an animal cage to the bodies of a group of free-moving laboratory rodents [16].

Wireless power transfer (WPT) in medical implanted devices (MIDs) has received significant interest from both academic and the medical industry. These systems have suffered from battery-life that must be charged or replaced. Also, some implant devices are large, leading them to be uncomfortable. In addition, the device may interact with internal tissues, which may lead to reactions that affect the patient. This paper aims to produce a small MID operated by WPT to transmit vital signs (i.e., temperature) to an external station to ensure that the device does not affect the patient's body. The proposed system used a flat spiral coil as a transmitter and a multi-layer copper wire coil as the receiver coil. The transmitter circuit was implanted inside a rabbit's body. The temperature of the rabbit was sent using the nRF24L01 transceiver to the external monitoring station. The system reached an efficiency and power of 23.37% and 1.98 W respectively on 50 Ω load resistors [17].

Biosensors devices have attracted the attention of many researchers across the world. They have the capability to solve a large number of analytical problems and challenges. They are future ubiquitous devices for disease diagnosis, monitoring, treatment and health management. This review presents an overview of the biosensors field, highlighting the current research and development of bio-integrated and implanted biosensors. These devices are micro- and Nano-fabricated, according to numerous techniques that are adapted in order to offer a suitable mechanical match of the biosensor to the surrounding tissue, and therefore decrease the body's biological response. For this, most of the skin-integrated and implanted biosensors use a polymer layer as a versatile and flexible structural support, combined with a functional/active material, to generate, transmit and process the obtained signal. A few challenging issues of implantable biosensor devices, as well as strategies to overcome them, are also discussed in this review, including biological response, power supply and data communication[18].

On duty cycling of the power transmission for millimeter-scale implants. In the proposed method, the power transmitter (TX) transmits the wave with a duty cycle. It transmits only during a short period of time and pauses for a while instead of transmitting

the wave continuously. In doing so, the TX power during the active period can be increased while preserving the average TX power and the specific absorption rate (SAR). Then, the incoming voltage becomes significantly larger at the rectifier, so the rectifier can rectify the input with a higher PCE, leading to improved PTE. To investigate the design challenges and applicability of the proposed duty-cycled WPT method, a case for powering a $1 \times 1\text{-mm}^2$ -sized neural implant through the skull is constructed. The implant a TX, and the associated environment are modeled in High-Frequency Structure Simulator (HFSS), and the circuit simulations are conducted in Cadence with circuit components in a 180-nm CMOS process. At a load resistor of $100\text{ k}\Omega$, an output capacitor of 4 nF , and a carrier frequency of 144 MHz , the rectifier's DC output voltage and PCE are increased by 300% (from 1.5 V to 6 V) and by 50% (from 14% to 64%), respectively, when the duty cycle ratio of the proposed duty-cycled power transmission is varied from 100% to 5% [19].

The research in [2] had evaluated and discussed a survey of popular methods for wirelessly transfer power into implantable medical devices. Power delivered in the reviewed works to medical implants varies from few μW to 5.4 W with a distance of 1 mm to 4 m and maximum efficiency of up to 79.6%. This paper provides a perspective on different WPT approaches for biomedical applications by investigating the significant works in this field. Also, some points for designing an effective implantable medical device and related commercial rules and regulations are presented.

Analytical and simulation approaches to link design and performance evaluation are explored for wireless power transmission system. Electrical parameters are extracted from geometric Parameters of the primary and secondary file and the two port network model Correlation design and performance evaluation were considered. Magnetic resonance coupling using SP configuration is specified for a longer distance in the MHz frequency range [20].

Wireless power transmission (WPT) is a critical technology that provides an alternative for wireless power and communication with implantable medical devices (IMDs). This article provides a study concentrating on popular WPT techniques for IMDs including inductive coupling, microwave, ultrasound, and hybrid wireless power

transmission (HWPT) systems. Moreover, an overview of the major works is analyzed with a comparison of the symmetric and asymmetric design elements, operating frequency, distance, efficiency, and harvested power. In general, with respect to the operating frequency, it is concluded that the ultrasound-based and inductive-based WPTs have a low operating frequency of less than 50 MHz, whereas the microwave-based WPT works at a higher frequency. Moreover, it can be seen that most of the implanted receiver's dimension is less than 30 mm for all the WPT-based methods. Furthermore, the HWPT system has a larger receiver size compared to the other methods used. In terms of efficiency, the maximum power transfer efficiency is conducted via inductive-based WPT at 95%, compared to the achievable frequencies of 78%, 50%, and 17% for microwave-based, ultrasound-based, and hybrid WPT, respectively. In general, the inductive coupling tactic is mostly employed for transmission of energy to neuro stimulators, and the ultrasonic method is used for deep-seated implants [21].

In this research wireless power transfer using near-field inductive coupling is studied and investigated. The focus is on delivering power to implantable biomedical devices. The objective of this research is to optimize the size and performance of the implanted wireless biomedical sensors by: (1) proposing a hybrid multiband communication system for implantable devices that combines wireless communication link and power transfer, and (2) optimizing the wireless power delivery system. Wireless data and power links are necessary for many implanted biomedical devices such as biosensors, neural recording and stimulation devices, and drug delivery and monitoring systems [22].

Wireless wearable sweat biosensors have gained huge traction due to their potential for noninvasive health monitoring. As high energy consumption is a crucial challenge in this field, efficient energy harvesting from human motion represents an attractive approach to sustainably power future wearables. Despite intensive research activities, most wearable energy harvesters suffer from complex fabrication procedures, poor robustness, and low power density, making them unsuitable for continuous biosensing. Here, we propose a highly robust, mass-producible, and battery-free wearable platform that efficiently extracts power from body motion through a flexible printed circuit board (FPCB)-based freestanding triboelectric Nano generator (FTENG) [23].

CHAPTER ONE INTRODUCTION

Wireless Power Transmission (WPT) (WPTS) Dynamic medicine is grown. WPTS consists of self-duplexing Pneumatic agricultural, efficient, and WPT transmitter (WPT TX). The proposed system is capable of working simultaneously Transfer of recorded data and recharge batteries Hardware (to prolong the agriculture). WPT TX is running the dimensions of 50 x 50 x 1.6 mm 3 are optimized for effectiveness Power transfer at 1470 MHz to 45 mm depth Device [24].

An approach to improve wireless power transfer (WPT) to implantable medical devices using loop antennas is presented. Antenna exhibits strong magnetic field and dense flux line distribution along two orthogonal axes by insetting the port inside the antenna area. The design shows excellent performance against misalignment in the y-direction and higher WPT as compared with a traditional square loop antenna. Two antennas were optimized based on this approach, one wearable and the other implantable. Both antennas work at both the ISM (Industrial, Scientific, and Medical) band of 433 MHz for WPT and the Med Radio (Medical Device Radio communications Service) band of 401–406 MHz for communications. To test the WPT for implantable medical devices, a miniaturized rectifier with a size of 10 mm × 5 mm was designed to integrate with the antenna to form an implantable rectenna. The power delivered to a load of 4.7 kΩ can be up to 1150 μW when 230 mW power is transmitted which is still under the safety limit. This design can be used to directly power a pacemaker, a nerve stimulation device, or a glucose measurement system, which requires 70 μW, 100 μW, and 48 μW DC power, respectively [25].

Conventional resonant inductive coupling wireless power transfer (WPT) systems encounter performance degradation while energizing biomedical implants. This degradation results from the dielectric and conductive characteristics of the tissue, which cause increased radiation and conduction losses, respectively. Moreover, the proximity of a resonator to the high permittivity tissue causes a change in its operating frequency if misalignment occurs. In this report, we propose a metamaterial inspired geometry with near-zero permeability property to overcome these mentioned problems. This metamaterial inspired geometry is stacked split ring resonator metamaterial fed by a driving inductive loop and acts as a WPT transmitter for an in-tissue implanted WPT receiver. The presented demonstrations have confirmed that the proposed metamaterial

CHAPTER ONE INTRODUCTION

inspired WPT system outperforms the conventional one. Also, the resonance frequency of the proposed metamaterial inspired TX is negligibly affected by the tissue characteristics, which is of great interest from the design and operation prospects. Furthermore, the proposed WPT system can be used with more than twice the input power of the conventional one while complying with the safety regulations of electromagnetic waves exposure [26].

CHAPTER TWO

WIRELESS POWERING OF BIOSENSORS

2.1 Introduction

Sensors represent a fast-growing field, as they have been shown to be very helpful in our daily life, playing roles in industries such as agriculture, food safety, homeland security, bioprocessing, environmental monitoring, and industrial monitoring. Beyond these, the application of biosensing in medicine and biomedical engineering may have the highest potential for growth and for affecting human quality of life in the near future. This potential is driven by the need for new and improved devices and technologies with improved sensitivity, specificity, reliability, and biocompatibility, which can solve and manage medical and health problems such as heart diseases, cancer, or diabetes, among others. For example, since tumors present a unique microenvironment, an implantable biosensor near a tumor would allow precise monitoring of the disease's progression. The first biosensor reported for use *in vivo* was based on magnetic nanoparticles and was used to detect soluble cancer biomarkers in mice [1]. In recent years, medical progress has evolved with an increased interest in instruments for sensing and controlling the specific functions of the brain. These medical instruments considerably decrease morbidity and improve the standard of life for certain patients. Sensor systems are now quite advanced but providing power to these devices is still a major challenge. The answer to this issue is using WPT technologies for a range of biomedical implants [2].

Wireless power transfers the technology that enables a power source to transmit electromagnetic energy to an electrical load across an air gap, without inter connecting cords. This technique is rapidly growing and is applicable to the domains, including industrial applications consumer products and biomedical implant. Biomedical implanted devices are becoming popular in health and medical applications in a wide range of areas, such as, cardiac pacemakers, retinal prosthesis, cochlear implants, defibrillator, smart orthopedic implants, and artificial hearts [20]. We can find sensors everywhere, and the whole world is full of sensors and their applications. There are many types of sensors available around us, in our offices, gardens, shopping malls, homes, cars, toys etc. These

sensors make our lives so easy and comfortable, starting from applications such as switching on the lights, fans, television (TV), automatic adjustment of the room temperature by air conditioning (AC), fire alarm, detecting obstacles when the car is reversing, making a thumb impression etc. A sensor is a device which receives signals as well as responding to a signal or stimulus. The stimulus signals can be defined by the measure, property, or state which is sensed. We also can say that a sensor is a translator that converts a nonelectrical value to an electrical value [3]. Summary of Wireless Power Solutions for Biomedical Devices We can categorize biomedical WPT into three areas: near-field, far-field, and the recently proposed “mid-field” [15]. A notable exception to this schema is ultrasound WPT, which transfers power through human tissue acoustically [11]. While this is certainly an interesting topic, analysis of ultrasound WPT systems is less developed than their electromagnetic counterparts. Ultrasound systems will not be considered for this work [9]. There are two main types of sensors: passive sensor and active sensor. A passive sensor does not require any extra energy source and electric signal is produced directly in reply to stimulus of external sources. This means that the sensor converts input energy to output signal energy [5]. Implantable biosensors need to consider the FBR, which implies the choice of biocompatible materials and fabrication methods. Therefore, biocompatibility and lifetime are the major limitations besides the power methodologies. Approaches for harvesting energy from the body environment have been investigated as an alternative to the conventional battery-based systems for powering the wearable and implantable biosensors[13]. The power consumption of an implantable biosensor is determined by many factors, such as its complexity, the nature of a sensed signal, the number of transmissions per second, and so on. Biosensors that consume less than 20 μ W, have already been reported [6].

2.2 Different Approaches for Wireless Power Transfer Systems

The lifespan of implantable medical devices is limited to battery capabilities. Patient pain and the danger of infection are the major development concerns in implantable medical systems because the use of implanted batteries can cause diseases. Therefore, the WPT link is a safer option to power biomedical implant. Typically, non-rechargeable batteries with greater weight and volume, and shorter period of

effectiveness compared to rechargeable batteries, are employed for implantable medical devices. Medical implants like implanted spinal cord stimulators can use a rechargeable battery to improve their capability and reduce overall. Lately, there is a great interest in the usage of the WPT for medical applications. The development of implantable electronic devices in a biological system made it easier to use this technology for powering various implantable medical devices such as biological sensors, pacemakers, and neurostimulator working in a range of power from a few microwatts to a few watts. As shown in Figure 2.1, the power ranges of common implantable medical devices are illustrated. The WPT system for the neurostimulators and the pacemaker are discussed in detail in respectively.

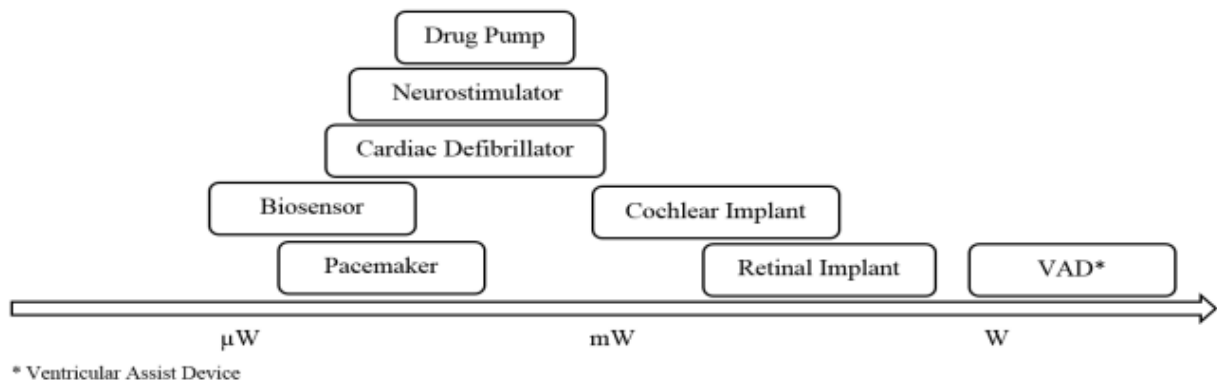


Figure 2.1. Power range of implantable medical devices.

There are reliability problems with the classic wireless power links. An option that facilitates the growth of bio-implants is the use of CMOS processes. The procedure is to include the standard CMOS with the implanted receiver. This reduces the cost, improves productivity, and provides compatibility and reliability of prototypes. The usage of CMOS for WPT systems are presented in. A backward communication unit transmits the information to an external data communicator using modulation. Typically FSK, PSK, ASK, OOK, LSK, PPSK, QMPM, QPSK, impedance modulation have been used for data communication units in medical applications. Long-term RF and microwave exposure is dangerous. The device layout must, comply with the associated safety regulations to protect patients from electromagnetic radiation damage. It is possible to

evaluate maximum permissible exposure (MPE) in environments for electromagnetic field intensity by assessing the specific absorption rate (SAR). IEEE Standard Basis C95.1 expresses SAR limitation. According to this principle, the maximum SAR value must be below 1.6 W/kg for any 1g of the body tissue and below 0.08 W/kg for the whole body. Nevertheless, the maximum SAR limitation is 4 W/kg for every 10 g of the tissue of the body parts such as the hands, feet, ankles, and wrists. Mainly, determining SAR can be achieved by using numerical techniques and empirical models using fabricated tissue phantoms. The maximum SAR value is studied in. The empirical results can be obtained, in vivo, using a living organism or in vitro, outside of a living organism. To mimic the biological effects of human body tissue, the phantom is very popular among researchers in this field. The tissue electromagnetic properties play an important role in the design of implantable devices. The assessment of variation on tissue electromagnetic properties was provided by Bocan et al. The recent reports on tissue electromagnetic properties are depicted in Table. 2.1 [2].

Table 2.1. Summary of different approaches in analyzing of tissue electromagnetic properties

Reference	Year	Tissue	Frequencies	Models/Methods
48	2020	in-vivo, ex-vivo	-	FEM*
49	2019	Muscle, fat, skin	50MHz, 300MHz, 700MHz and 900MHz	FDTD**
50	2019	Body	(0.5-26.5) GHz	Measured properties, Cole-Cole
51	2018	Brain, liver	200-1600 Hz	Measured properties
52	2018	Muscle, fat, skin	915 MHz and 2 GHz	Measured properties
53	2017	Blood, liver, fat, and brain	10 kHz-10MHz	Bottcher-Bordewijk model, Measured properties
54	2016	Muscle, bladder, cervix	128 MHz	Measured properties, Cole-Cole
55	2016	Body/14 tissues	2.1 GHz, 2.6 GHz	FDTD
56	2016	Head	(0.75 – 2.55) GHz	Phantom/ FEM
57	2016	Muscle	500 MHz- 20 GHz	Fricke
58	2015	Eye/6 tissues	(0.9 – 10) GHz	FDTD
59	2015	Skin	(0.8 – 1.2) THz	FEM
60	2014	Eye, head/14 tissues	(0.9 – 5.8) GHz	FDTD
61	2010	Head	-	FEM
62	2009	Head/16 tissues	50 MHz- 20 GHz	Measured properties, FDTD
63	2006	Eye, head/15 tissues	900 MHz, 1800 MHz, 2450 MHz	FDTD
64	2004	Body	400 MHz, 900 MHz, 2400 MHz	Visible human, FDTD
65	2004	Body/51 tissues	30 MHz- 3 GHz	FDTD
66	2002	Head/10 tissues	900 MHz, 1800 MHz	Visible human, FDTD

* Finite Element Method

** Finite-Difference Time-Domain

2.3 Principles of WPT Systems

Wireless power transfer (WPT) system can be categorized into far field and near field WPT. The far field WPT system is categorized into LASER, Photoelectric, RF, and Microwave while inductive coupling, magnetic resonance coupling and capacitive coupling based methods are categorized into near field WPT system. Inductive coupling is based on magnetic field induction that delivers electrical energy between two coils without external resonating capacitor. The operating frequency of inductive coupling is typically in the kHz range. The secondary coil should be tuned at the operating frequency to enhance charging efficiency, while Magnetic resonance coupling is based on evanescent-wave coupling which generates and transfer electrical energy between two resonant coils through varying or oscillating magnetic fields. As two resonant coils, operating at the same resonant frequency are strongly coupled, high energy transfer efficiency can be achieved. Figure 2.2 shows the general flow diagram of wireless power transfer system for biomedical implant and Figure 2.3 shows the different resonant configurations for resonant inductive coupling. In this work, magnetic resonant coupling using series-parallel (SP) resonant configuration is discussed [20]. As magnetic resonance coupling typically operates in the megahertz frequency range, the quality factors are normally high. With the increase of charging distance, the high quality factor helps to mitigate the sharp decrease in coupling coefficient, and thus charging efficiency. Consequently, extending the effective power transfer distance to meter range is possible [3]. A two port network as shown in Figure 2.4 is obtained by extracting electrical parameter from geometrical parameter, where the primary coil (L_1) is driven by a power source and the secondary coil (L_2) connected to a load, which is embedded in implant. From Figure 2.4 the link impedance (Z_{link}) is the impedance looking into the link and output impedance (Z_{out}) is the impedance connected to the output port of the link [20].

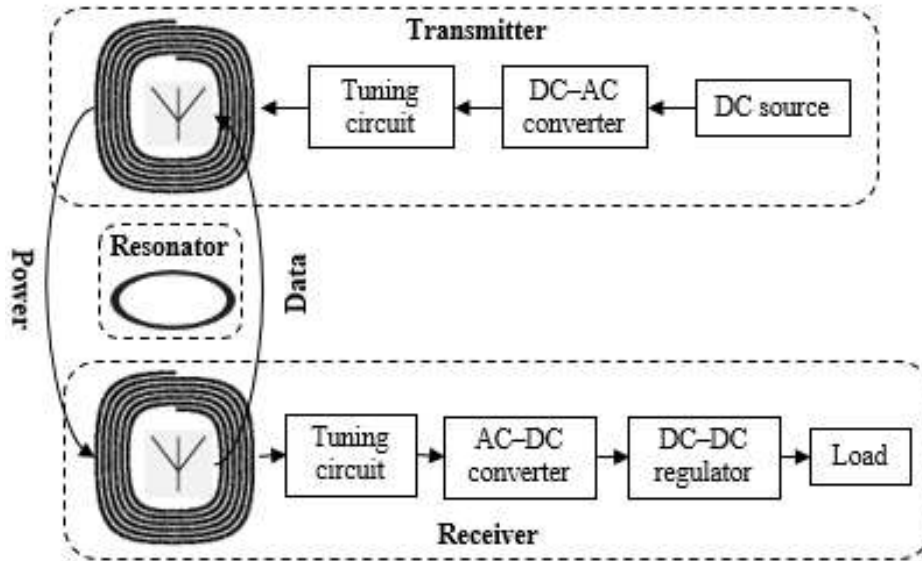


Figure 2.2. General diagram of WPT for biomedical implants.

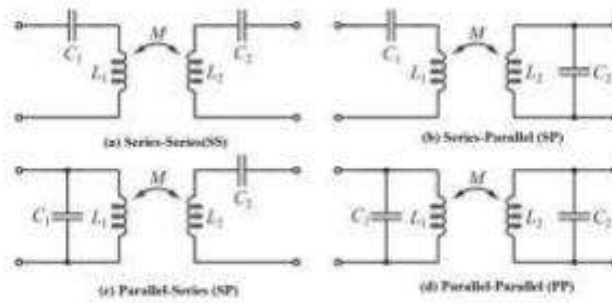


Figure 2.3. Different resonant configurations for magnetic resonant coupling.

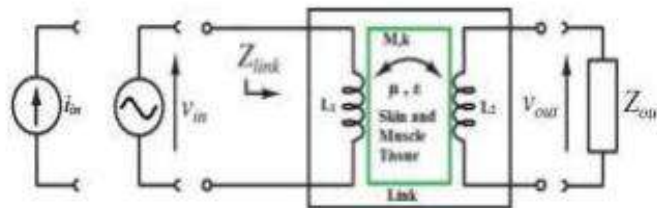


Figure 2.4. General two port network model of extracted electrical parameters.

2.4 Mat-Based Wireless Power Transfer to Moving Targets

Neural stimulation and recording provide emerging prosthetic and treatment options for spinal cord injury, stroke, sensory dysfunction, and other neurological diseases and disorders. Neural recording from awake animals with observable behavior has greatly enhanced our understanding of central and peripheral nervous systems. Although there has been substantial studies on miniaturized, implantable electronic circuits that record neural data and stimulate neuronal networks in freely moving laboratory animals, the mobility of the animal subject is often limited, and the experimental results obtained under restricted conditions may not reflect the full repertoire of brain activity corresponding to their natural behaviors. There are similar problems in the study of new drugs which often requires monitoring a number of variables from the inside of the animal body and observation of their mobility and behaviors. Traditionally, magnetic induction was used for WPT using a similar form to a transformer. This form of the magnetic induction method is highly efficient (>90%) in the near-field range, but much less efficient as the transmission distance increases. In 2007, an efficient mid-range WPT via strongly coupled magnetic resonance was reported. This system consists of four coils (Figure 2.5), namely, driver, primary (or transmitter), secondary (or receiver), and load coils. Inductive coupling is used between the driver and primary coils as well as between the secondary and load coils. The primary and secondary coils with the same resonant frequencies tend to exchange energy efficiently. This mechanism is valuable in the application to medical implants because biological tissues are generally nonresonant at the operating frequency in the RF range. Because our special WPT system involves moving targets (animals, e.g., rodents), the vertical component of the magnetic field generated by the transmitter is required to be distributed as even as possible over the entire area of interest (e.g., floor of the rodent cage). When this condition is satisfied, the device carried by or implanted within each rodent can receive steady power at any location of the floor. Previously, we designed a WPT system in which multiple circular spiral coils were printed on hexagonal PCBs. These PCBs were then tiled hexagonally forming a “power mat” shown in Figure 2.6. Note that the use of hexagons in the pack of coils is not an arbitrary choice, rather it has been proven that this design will leave the smallest gap between circular resonator coils. The power mat is able

to deliver wireless power to the implants and “carry-on” devices to multiple rodents which move freely on the floor above the mat [15].

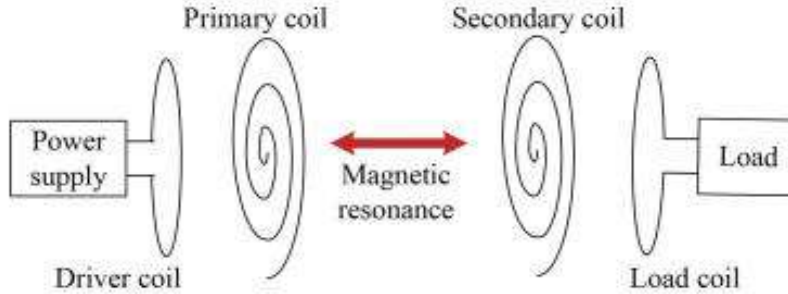


Figure 2.4. A resonance based WPT system including four coils.

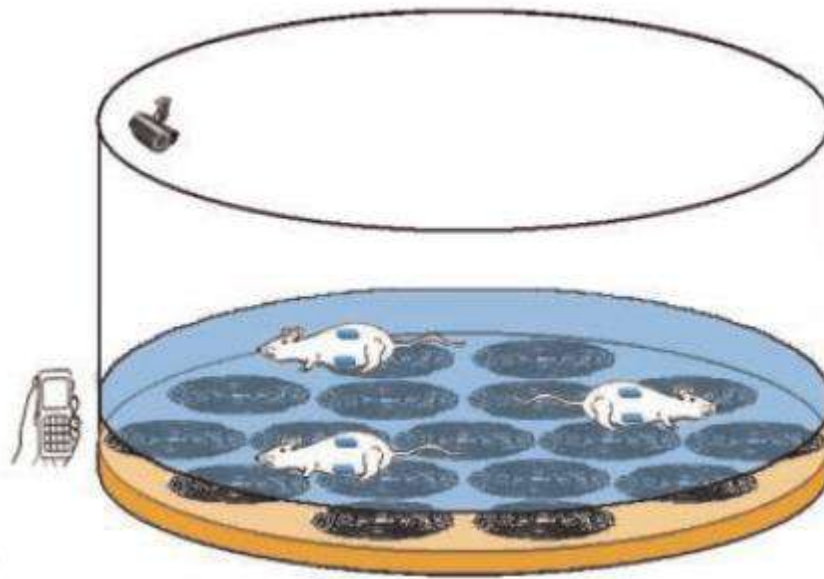


Figure 2.5. WPT system in which the floor of the animal cage is located over a hexagonally packed power mat.

2.5 The Categories of Wireless Power Transfer

The categories are classified based on the working distance, d , between the transmitter and receiver, in the wireless power transfer system in Figure 2.6.

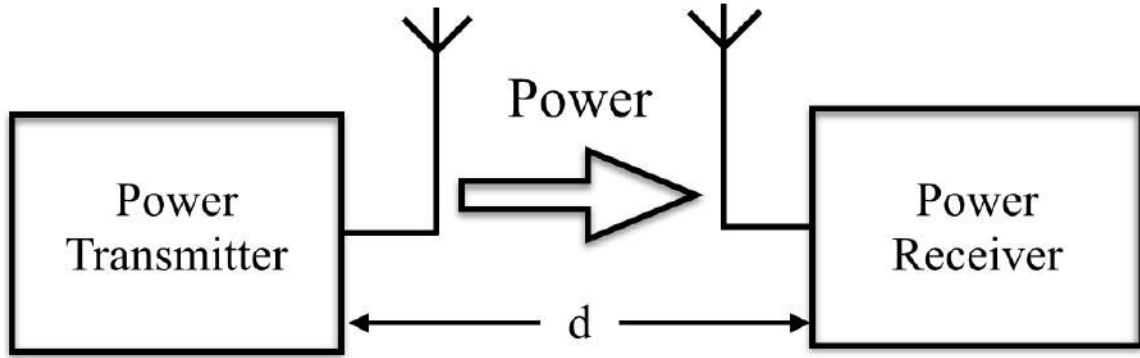


Figure 2.6. The block diagram of wireless power transfer system [7].

The illustration of these categories is shown in Figure 2.7. Suppose the wavelength of power transfer is λ , and the transmission distance d is less than $\lambda/2\pi$, $d < \lambda/2\pi$, then the system is classified as near field. If d is more than λ/π , $d > \lambda/\pi$, it is named as far field. The mid field is classified as d between $\lambda/2\pi$ and λ/π , which is $\lambda/2\pi < d < \lambda/\pi$.

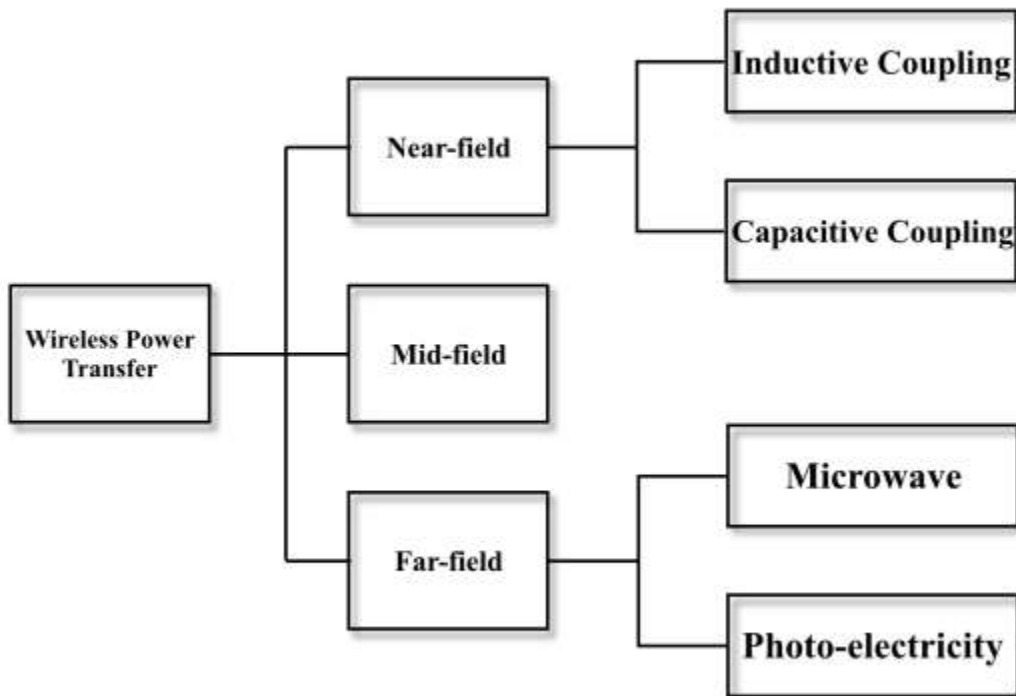


Figure 2.7. The categories of wireless power transfer techniques [7].

2.5.1 Near Field Wireless Power Transmission

In near field WPT, the basic power transmission approaches are magnetic induction and electric induction. The next paragraphs will describe them separately. Wireless power transfer through electric induction uses capacitive power transfer (CPT) technique. Due to its small system volume and profile, CPT is used in small sized applications such as biomedical applications, robots and mobile devices. In addition, the merits of a cheap and flexible design make the capacitive power transfer to be an appropriate method in moving systems, such as robot arms.

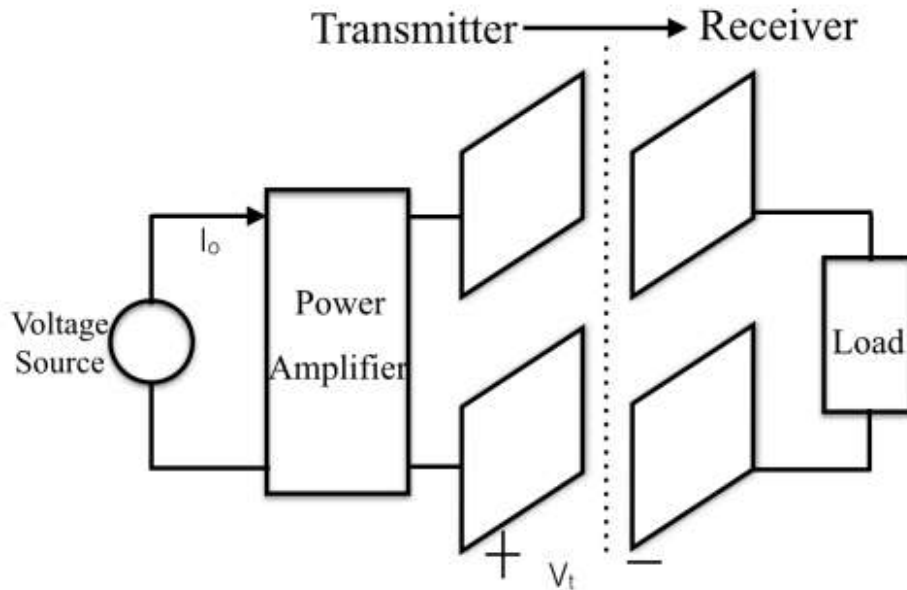


Figure 2.8. The topology of capacitive wireless power transfer system.

Even though the magnetic induction has the advantage of high power transfer efficiency than capacitive power transfer, CPT is the better choice than the magnetic induction under the high operational frequency scenarios. The basic topology of CPT system is shown in Figure 2.8. The power amplifier is usually adopted as an inverter. This inverter is utilized to generate AC signal and feeds the signal through a capacitive interface. The power can then be transferred via the system to the load. The capacitance is typically few hundreds Pico farads in value. To feed enough current to the interface, in certain systems, inductors are placed before the capacitors. The existing capacitive power

transfer systems use large capacitors. The operation theory of capacitive power transfer technique is described as follow. The alternating voltage signal, which is generated from the power supply and the power amplifier, is applied to the capacitor. It produces an electric field which can be modeled as [7]:

$$E = \frac{V}{l}. \quad (2.1)$$

Here, V is the voltage applied on the two plates of the capacitor and l is the distance between the two plates. The alternating voltage will induce an oscillating electric field in the capacitor. Due to the electrostatic induction, the alternating electric field can generate a variable potential on the receiver plate. Thus, an alternating current is also generated to feed the load. The transmitted power depends on the frequency and capacitance. In Figure 2.7, the power which is going to be transferred to the load is expressed as [14]:

$$P = V_t I_o \cos(\beta). \quad (2.2)$$

In 2.2, V_t is the voltage across the two plates of transmitter capacitor and β is the phase difference between the voltage V_t and the transmitter current I_o . β and I_o can be derived as [7]:

$$\beta = \tan^{-1}\left(-\frac{1}{\omega C R_{re}}\right), \quad (2.3)$$

$$I_o = \frac{V_t}{\sqrt{(1/\omega^2 C^2) + R_{re}^2}}, \quad (2.4)$$

Where, C is the capacitance, ω is the working frequency and the R_{re} is the reflected impedance in the transmitter which is from the receiver. Then the voltage across each capacitor then is found as:

$$V_C = \frac{I_o}{\omega C}. \quad (2.5)$$

Equations (2.2)-(2.5) present the important design parameters. These design factors can be optimized to achieve the best working condition of CPT system.

Currently, CPT is applied in some low power applications. For applications involving high power transfer, the magnetic induction will be used. Additionally, electric fields can interact strongly with some materials, such as human muscle. Therefore, for powering biomedical implants, the magnetic induction is more widely used instead of electric induction.

Magnetic Induction Power Transfer (MIWPT [7]) is used to transfer power via magnetic field. The magnetic coupling can be defined as two groups, inductive wireless power transfer (IWPT) and resonant wireless power transfer (RWPT). The inductive wireless power transfer is realized by utilizing non-resonant coupled inductors, such as a conventional transformer. It works on the principle of a primary coil generating a magnetic field due to an AC current and inducing an alternating voltage in the receiver coil. This technique requires that the magnetic field is covered by the receiver coil in short distance and the presence of a magnetic core is necessary. The coupling between the two coils is determined by the distance between the inductors, the shape and the placement angle of the coils. The working theory of this technique is shown in Figure 2.9. Here, L_1 represents the transmitter coil which is typically to be made as large as possible for transmitting more power. L_2 is the receiver coil to receive the energy. B indicates the magnetic field coupled by the two coils and Z is the distance to transfer the power.

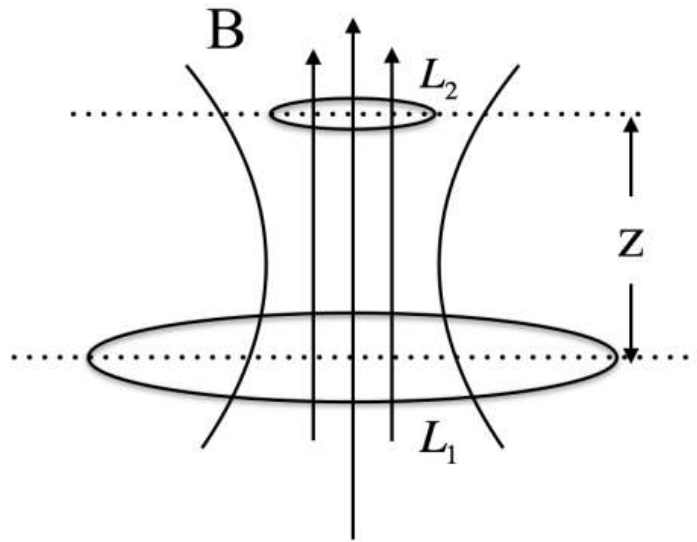


Figure 2.9. Conceptual illustration of the inductive coupling wireless power transfer technique.

The resonant coupling method is considered to be the most efficient way in wireless power transfer applications. This method requires a resonant transformer. As for the basic two resonator system, it has two high quality factor Q coils connected with capacitors to form two coupled LC circuits. This structure is shown in Figure 2.10. The resistors R_S and R_C are used to model the parasitic resistors associated with the coils L_S and L_C , respectively. If these two resonators are placed in proximity to one another such that there is magnetic coupling between them, it becomes possible that the resonators can exchange the energy in high efficiency. When the two resonators work at the same resonant frequency, the energy transfer efficiency can be maximized. In resonant wireless power transfer, an oscillating current is passed through the coils. This current will induce an oscillating magnetic field too. Under the highly resonant situation, the energy is stored in the coils. The biggest disadvantage of non-resonant coupled inductors is the power decaying more server than resonant coupled coils. By using the inductive coupling wireless power transfer, the distance between the two coupled coils needs to be as close as possible. While, using the resonance, this disadvantage can be eliminated, resulting in the improvement of power transfer efficiency. The power transfer efficiency is highly depended on the coupling factor between the two coils. The system can be mainly classified as four categories based on the coupling coefficient. First is the tight coupling, meaning that the coupling factor is around 1. Second is the over coupling, it happens when the secondary coil is placed so close to the primary coil. The third category is defined as critical coupling. It happens when the power transfer is in its optimum passband. The last category is the loose coupling. It can be seen from its name that in this situation, the coils are far away from each other and the coupling coefficient is much less than the tight coupling. There are different structures to build the resonant wireless power transfer.

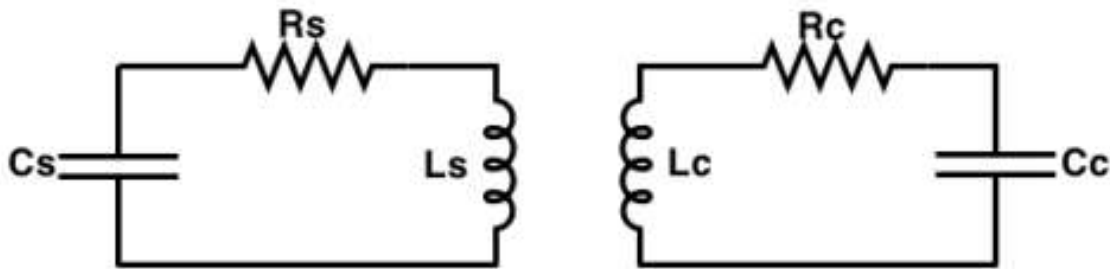
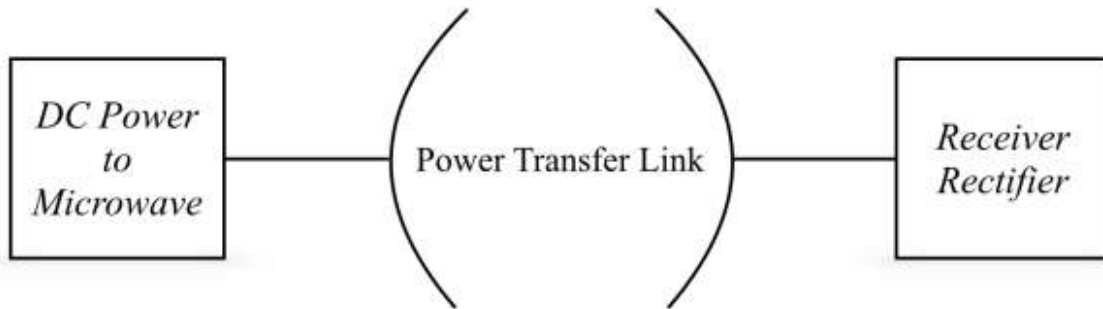


Figure 2.10. Resonance based wireless power transfer structure.**2.5.2 Far Field Wireless Power Transmission**

For achieving power transmission over large distances, the far field wireless power transfer technique is used. It is briefly introduced in this section. Two methods are usually adopted in far field transmission which are microwave and optical electricity.

Microwave Transmission uses microwave to transmit power over a long distance. This technique should thank to Nikola Tesla who contributed to the design of modern electricity supply system and demonstrated 'the power transmission without wires'. Basically, this power transmission technique can be divided into three blocks as shown in Figure 2.11. First block is to convert DC power to microwave power for making it to be ready transferred. The second block is the link which is used to transfer the power [7].

**Figure 2.11. Structure of microwave wireless power transmission system.**

The last one is the receiver block to receive and rectify the power. These blocks with their interaction determine the power transfer efficiency of the system. For example, if the power transfer efficiency of each block in Figure 2.11 is represented by η_1 , η_2 and η_3 , the overall power transfer efficiency can be found as:

$$\eta = \eta_1 \eta_2 \eta_3. \quad (2.6)$$

Optical Electricity which uses laser beam, is considered to be another promising approach for realizing the far field wireless power transfer. Even though the power is

transmitted using laser, in the receiver side the power still needs to be converted to the electrical energy. There are several advantages for utilizing laser for power transmission.

2.5.3 Mid Field Wireless Power Transmission

The power transfer distance of mid field is between near field and far field. It has been approved that it will generate high power transfer efficiency in mid field comparing to near field when the receiver dimension is less than the transmitter [7]. Conventionally, most of the research in near field wireless power transfer using magnetic field are based on applications that use a frequency less than 10 MHz. However, when the receiver size is much smaller than the transmitter, it results in a weak coupling and hence the inductively coupled coils are inefficient at the lower frequency. Therefore, in [7], it was shown that by utilizing a combination of inductive and radiative modes, higher power transfer efficiency can be achieved in mid field. Also, higher efficiency is achieved by utilizing in low-giga hertz range. However, in mid field wireless power transfer technique, one of the design difficulties is the voltage source for achieving optimum power transfer efficiency.

2.6 Resonant Coupling Wireless Power Transfer Structures

In resonance coupling, there are mainly 3 structures: two-coil links, three coil links and four coil links based on the number of coils used. These three structures are widely used in near field wireless power applications.

2.6.1 Two-Coil Based Wireless Power Transfer Structure

The two-coil based resonance coupling structure is shown in Figure 2.12. A voltage source is added at the transmitter with a source resistor R_S . On the transmitter side, the resonator is formed by a capacitor C_1 and the primary coil L_1 . There is also a parasitic resistor R_1 , the primary coil at the transmitter side. The receiver resonator is also formed by a capacitor C_P and the inductor L_2 . R_2 is the parasitic resistor of L_2 . The load is modeled by a resistor R_L .

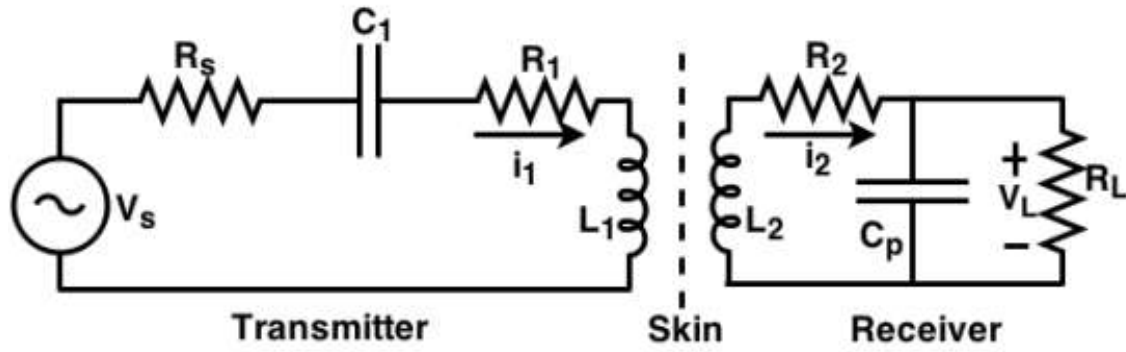


Figure 2.12. Circuit diagram of 2-coil wireless power transfer structure.

The current i_1 which goes through the transmitter coil is a time variant current. It generates a magnetic field. Through the mutual inductance M_{12} between the primary and secondary coil, the magnetic field goes into L_2 and generates the receiver current i_2 . The power is transferred by this mechanism. To maximize the transferred power, the working frequency of the transceiver LC resonators needs to be tuned to match each other. The frequency f_o is the resonance frequency of these two resonators:

$$f_o = \frac{1}{2\pi\sqrt{L_1C_1}} = \frac{1}{2\pi\sqrt{L_2C_p}}. \quad (2.7)$$

In Figure 2.12, the voltage across the load V_L can be expressed as [7]:

$$V_L = \frac{j\omega M_{12}i_1}{1 + (j\omega L_2 + R_2)\left(\frac{1}{R_L} + j\omega C_p\right)}. \quad (2.8)$$

2.6.2 Three-Coil Based Wireless Power Transfer Structure

The motivation of designing the three-coil structure is to achieve a high power delivered to the load without hurting the power transfer efficiency because as it will be seen, the four-coil based structure can reach a high power transfer efficiency but resulting in a low power received by the load. Comparing with the two-coil structure, an additional resonator is added between the transmitter and receiver to form three-coil power transfer structure. The circuit diagram of three-coil structure is shown in Figure 2.13.

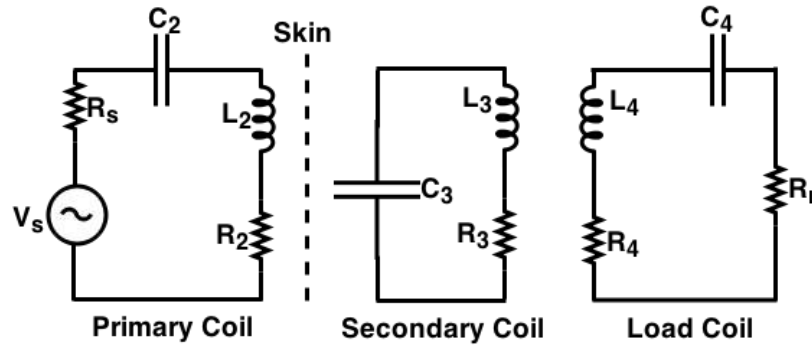


Figure 2.13. Circuit diagram of 3 coil wireless power transfer structure.

2.6.3 Four-Coil Based Wireless Power Transfer Structure

Comparing with the 3-coil structure, four-coil links is achieved by adding another additional resonator between the transmitter coil and receiver coil. It can mitigate the adversely effect of the small coupling factors between the transceiver. The basic four-coil structure is shown in Figure 2.14 [7].

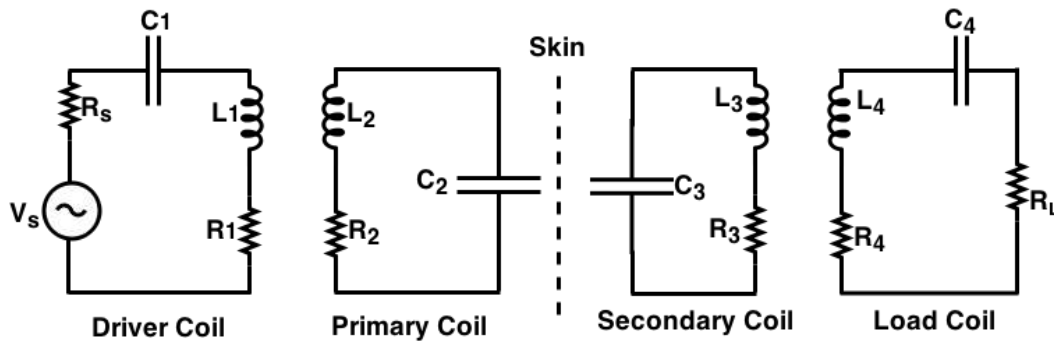


Figure 2.14. Circuit diagram of 4 coil wireless power transfer structure.

2.7 Implantable Biomedical Devices for POC Diagnostics

The field of implanted medical devices for point-of-care (POC) is turning into one of the most profitable businesses in USA, as these devices possess great advantages over their classical counterparts, since they offer better improvements to the quality of life of patients with chronic diseases, condemned to permanent and daily use of bio-analytical and invasive tests. Hitherto, many implantable devices have been approved by the FDA for a variety of applications ranging from monitoring of the glycemc index to the detection of heart and brain electrical imbalances and palliation of hearing malfunctions

[5]. In the beginning, the main role of implanted devices was to replace a missing biological structure through use of prosthesis such as artificial hearts or support damaged anatomical structures like arteries through the use of stents. Hence, as a natural continuation in this field, miniaturized implantable biosensors for point-of-care diagnostics of diseases come about as the new generation of implantable medical devices that feature higher measurement sensitivities of physiological parameters (Figure 2.15). As shown in Figure 2.15, Wireless Bio-Sensors (WBSs) can be classified in three groups including, wearable, handheld and implantable devices suitable for the detection of various diseases. Among these, depicted in Figure 2.16A–E, are the commercially available devices for management of brain and heart diseases. In these devices, as seen in Figure 1, analysis of the recorded signals can for instance, predict the onset of an epileptic seizure and accordingly stimulate the brain from the internal surface of the skull or directly in the deep brain. The recorded signal can be transmitted wirelessly as shown in Figure 2.16E, F. A similar technique is also being employed in novel heart pacemakers. Indeed, it was recently announced that a new pacemaker technology that uses electrical stimulation allows for making miniaturized devices that could be implanted in a minimally-invasive way and most importantly, the wireless device senses heart electrical activity and stimulates it without resorting to the use of leads, as shown in Figure 2.16 B, C. As, to the recording of brain electrical activity, the latter is sensed and the resulting electrical signal could be used for brain stimulation purposes for different diseases such as epilepsy and Alzheimer's. The main technical challenge in such bio-sensing devices is the type and number of electrodes. Ideally, the ability to access a number of cells around the brain individually can open several research avenues in the study of diseases that affect the Central Nervous System (CNS). However technically, this is not possible due to the damage inflicted to cells by electrodes. Therefore, the main tendency in device manufacturing, when using the current technology, strives to improve the conductivity at the electrode-tissue interface, using for instance, novel materials such as carbon nanotubes or nanowires. Also, the functionalization of said electrodes for selectively detecting other factors such as pH or glucose is another sought and important goal.

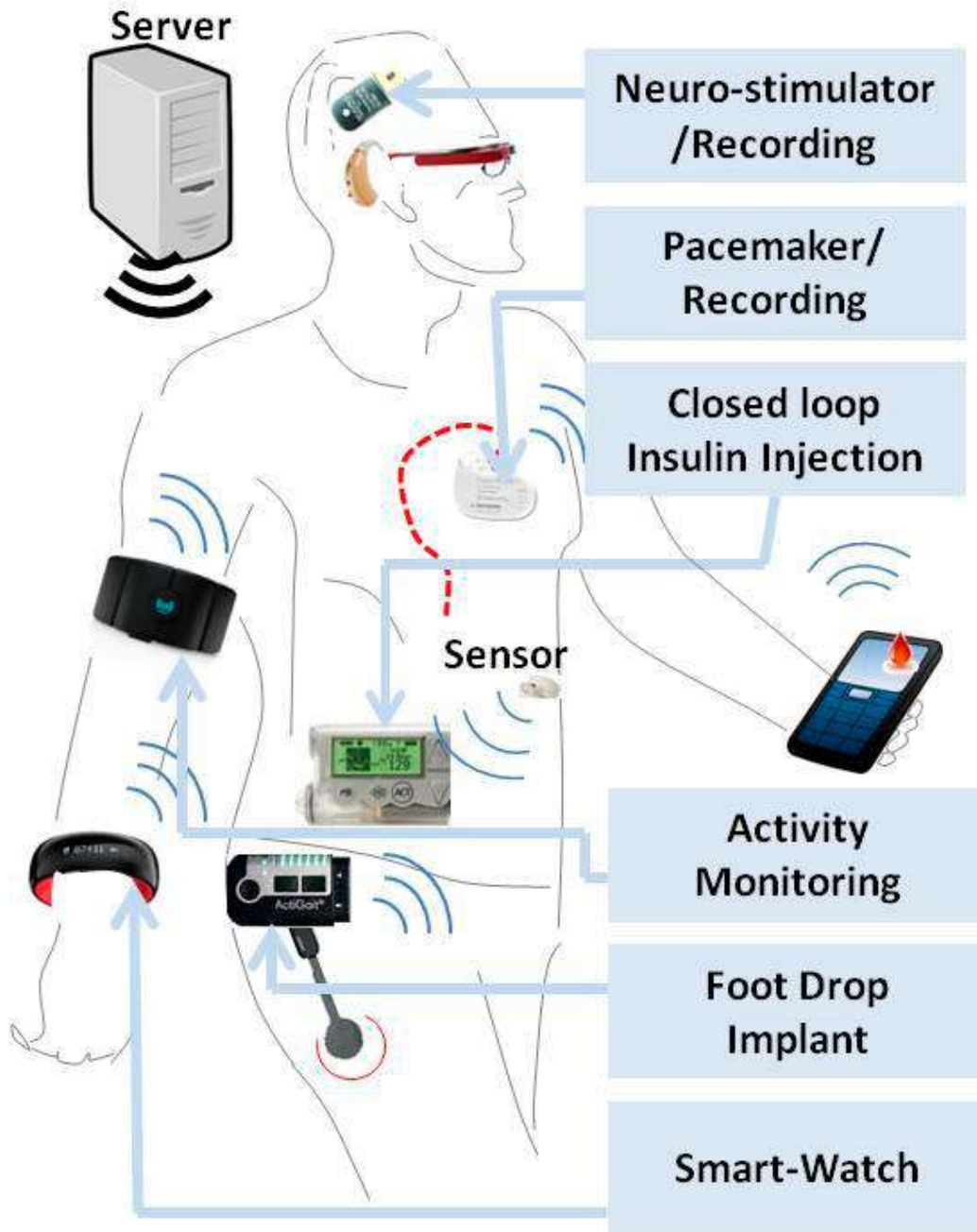


Figure 2.15. WBS technology for POC diagnostics of various diseases.

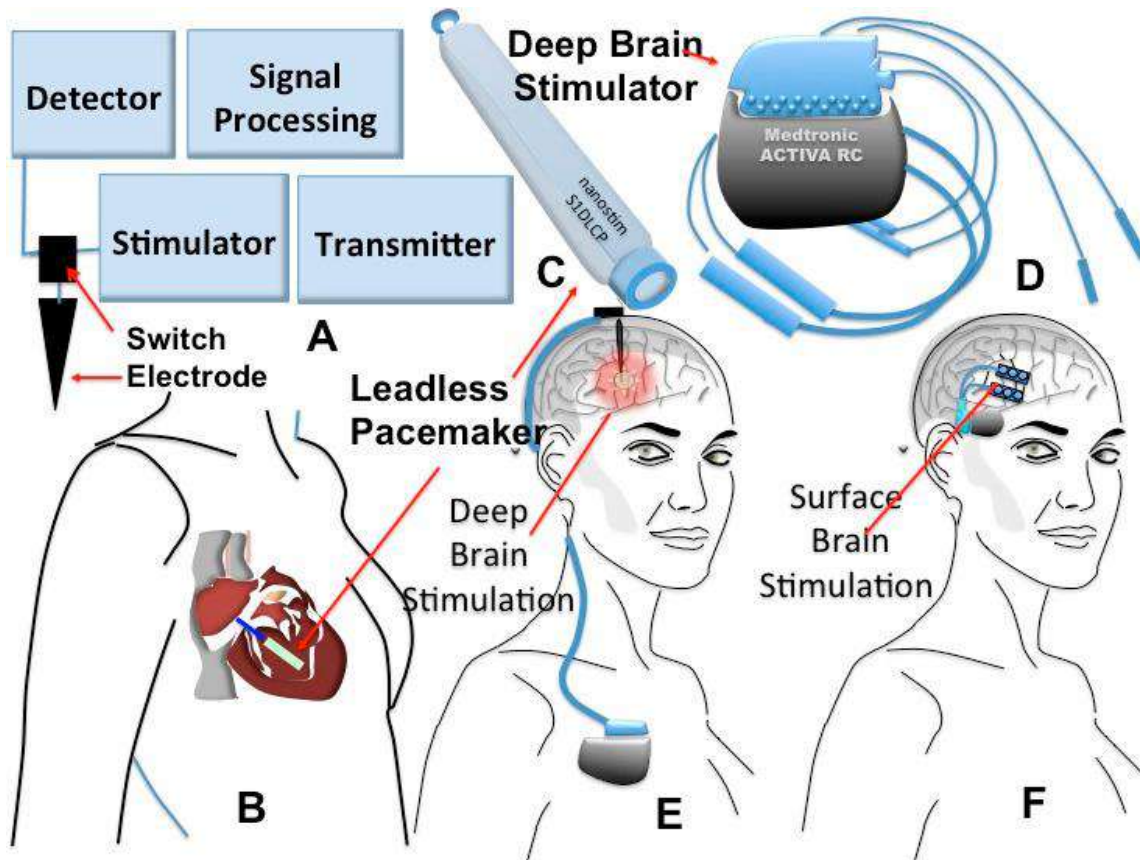


Figure 2.16. State of the art implantable devices for brain POC applications: (A) simplified diagram of implantable system; (B) the schematic of new wireless pacemaker placed in the heart; (C) the photo of this leadless pacemaker commercialized by Nanosim Inc.; (D) brain stimulator commercialized by Medtronic for epilepsy point-of-care purposes implanted; (E) under the skull for surface brain stimulation or (F) the stimulator placed above the chest for deep brain stimulation [5].

2.8 General Wireless Power Transmission (WPT) system

Figure 2.17 shows an overall circuit diagram of a general WPT system, which includes a transmitter (TX), receiver (Rx), and biological tissue in between. The two coils, L_1 and L_2 , are inductively coupled with a coupling coefficient k . The LC tanks on both sides are tuned to resonate at the same resonant frequency with C_1 and C_2 , respectively. The LC tank on the secondary side is connected to a rectifier, which generates a DC voltage V_{DC} , OUT to the load R_L . The figure also illustrates voltage waveforms of major nodes (V_{L1} , V_{L2} and V_{DC} , OUT) for the conventional and the proposed power transmission methods. As compared to the conventional WPT method

where the power is continuously transmitted, in the proposed duty-cycled power transmission, the RF power signal is transmitted during a designated portion of time only and remains dormant for the rest of the duration. The active and dormant periods are iterated with a periodic interval of T_I , as shown in Figure 2.18. Figure 2.18 shows the relationship between T_I and the active duty period (T_D) of the duty-cycled waveform. The ratio of these two is the duty cycle ratio D [19].

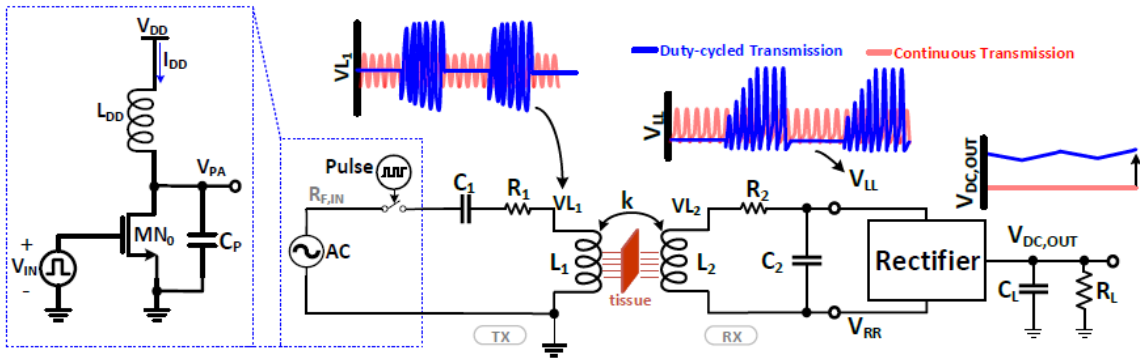


Figure 2.17. Circuit diagram of the general wireless power transmission (WPT) system with waveforms of major voltage nodes for the conventional continuous power transmission (in red) and the proposed Duty-cycled power transmission (in blue). Inset: Implementation scenario with a class-E amplifier for the input voltage control [19].

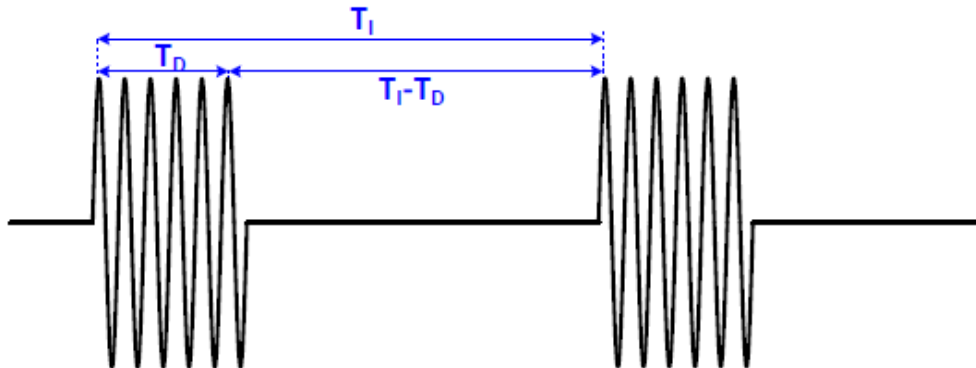


Figure 2.18. Duty-cycled waveform with indications of the duty cycle interval T_I and the active duty period T_D .

CHAPTER THREE

THE PROPOSED WPT SYSTEMS

3.1. Introduction

In this work, a wireless power transmission system using inductive coupling is proposed. The design of the resonant inductive WPT is carried out using the analytical method, which is incorporated in three constraints. The first one is the wireless power interconnection design, which is restricted by the size of the receiving in its corresponding implant. The second constraint is the design geometry of receiving and transmitting coils, while the third constraints is the modelling of the inductive link. In this work, planar spiral coils are exploited in the transmitting and receiving sides of the inductive link.

3.2. Design of Planar Spiral Coils

Figure 3.1 shows the planar spiral coil. Its inductance L_{Spiral} can be given by [27]

$$L_{Spiral} = \frac{\mu_0 n^2 d_{avg}}{2} \left(\ln \left(\frac{2.46}{\beta} \right) + 0.2\beta^2 \right) \quad (3.1)$$

Where, $\beta = (d_o - d_i)/(d_o + d_i)$ and is the fill-factor. μ is the permeability and it is equal to $\mu_0 \mu_r$. μ_0 is the absolute permeability and n is the number of turns. The average diameter is denoted by $d_{avg} = 0.5(d_o + d_i)$.

The DC resistance R_{DC} of any coil is given by

$$R_{DC} = \frac{l_c}{\sigma A_c} \quad (3.2)$$

Where, σ is the conductivity of the conductor, A_c is its cross-sectional area, and l_c is its length, which is determined as

$$l_c = \pi d_{avg} n \quad (3.3)$$

For planar spirals d_{avg} is given by [27]

$$d_{avg} = d_i + \frac{(w+s)n}{2} \quad (3.44)$$

Where, w is the conductor diameter and s the separation between each two adjacent turns.

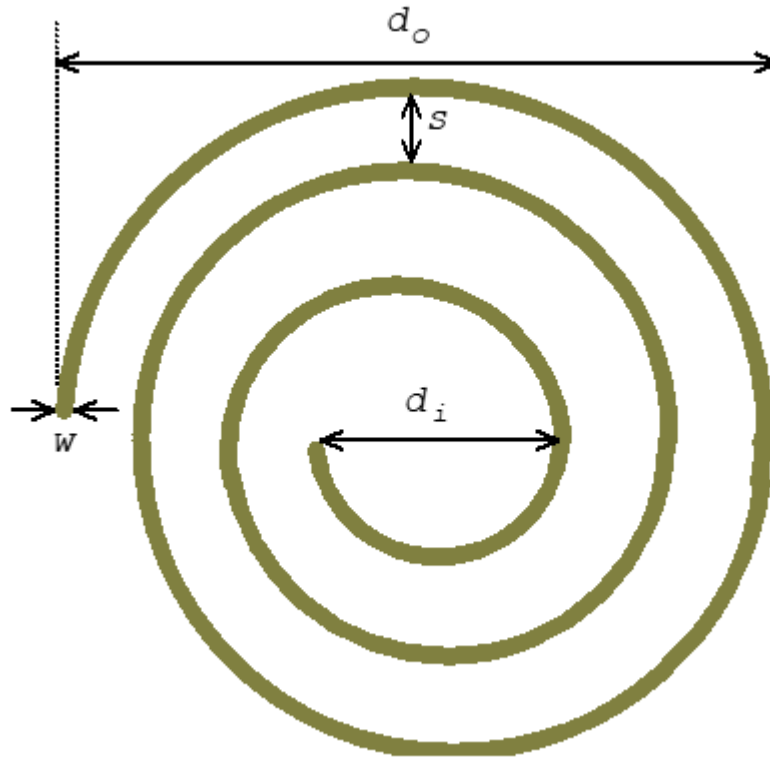


Figure 3.1. The planar spiral coil.

The coil AC resistance is given by [28]

$$R_{AC} = R_{DC} \frac{w}{2\delta} \quad (3.5)$$

Where, δ is the skin depth and is given by

$$\delta = \frac{1}{\sqrt{\mu\pi\sigma f}} \quad (3.6)$$

It is obvious that R_{AC} is proportional to the square root of the operating frequency f .

3.3. The Inductive Link

The inductive link can be modeled as shown Figure 3.2. The mutual coupling or mutual inductance M is defined by [27]

$$M = k\sqrt{L_1L_2} \quad (3.7)$$

Where, k is the coefficient of coupling between transmitting and receiving coils. L_1 and L_2 are the inductances of transmitting and receiving coils, respectively. Z_2 is a parallel or series combination of Load impedance Z_L and tuning capacitance C_2 . E_{ind} is an induced voltage in the secondary (receiving) side of the inductive link due the mutual effect of i_1 , which represents the current flowing in the primary (transmitting) side. Z_{refl} is an impedance reflected in the primary side due to mutual effect of the current i_2 flowing in the secondary side.

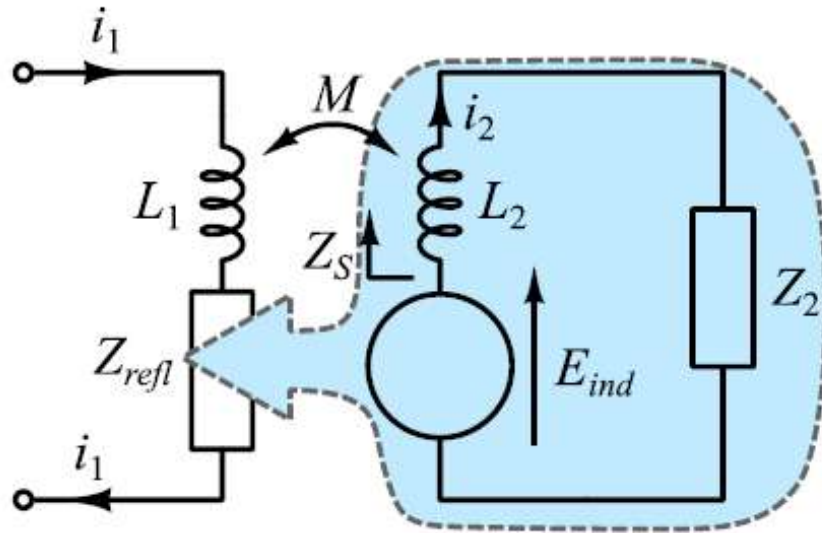


Figure 3.2. The Simplified model of an inductive link [27].

The reflected impedance Z_{refl} in the primary side is given by [27]

$$Z_{Ref1} = \frac{(\omega M)^2}{Z_S} \quad (3.8)$$

Where, ω is the power source angular frequency and is equal to $2\pi f$. Z_S is the impedance seen by the voltage source E_{ind} and it can be given by [27]

$$Z_S = j\omega L_2 + R_2 + Z_2 \quad (3.9)$$

Where, R_2 is the AC resistance corresponding to L_2 . The induced voltage source E_{ind} is defined by [27]

$$E_{ind} = -j\omega M i_1 = i_2 Z_2 \quad (3.10)$$

The link input impedance Z_{Link} can be given by

$$Z_{Link} = j\omega L_1 + R_1 + Z_{Ref1} = j\omega L_1 + R_1 + \frac{(\omega M)^2}{j\omega L_2 + R_2 + Z_2} \quad (3.11)$$

Where, R_1 is the AC resistance corresponding to L_1 . If the primary tuning capacitance C_1 is included in link model, then the link impedances for different arrangements of inductive link are calculated in Table 3.1 [27]. For SS and PS links, the output voltage v_{out} can be defined in terms of E_{ind} as follows:

$$v_{out} = \frac{E_{ind} Z_L}{j\omega L_2 + R_2 + \frac{1}{j\omega C_2} + Z_L} \quad (3.12)$$

And for SP and PP links:

$$v_{out} = \frac{E_{ind} Z_L}{(j\omega L_2 + R_2)(j\omega C_2 Z_L + 1) + Z_L} \quad (3.13)$$

For SS and SP links and according Figure 3.3, E_{ind} can be determined in terms of i_1 as follows:

$$i_1 = \frac{v_{in}}{Z_{Link}} \quad (3.14)$$

And for PS and PP links:

$$i_1 = \frac{i_{in} Z_{Link}}{j\omega L_1 + R_1 + Z_{ref1}} \quad (3.15)$$

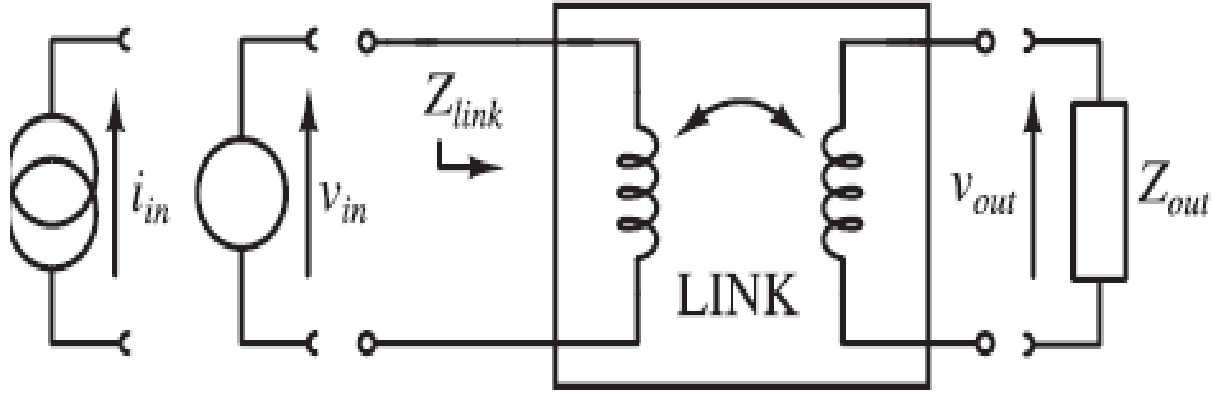


Figure 3.3. Two-port modeling of an inductive link excited either by voltage source or current source [27].

For all four topologies, the link voltage gains can be given by

$$A_{SS} = \frac{v_{out}}{v_{in}} = \frac{-j\omega M Z_L}{Z_{Link} \left(j\omega L_2 + R_2 + \frac{1}{j\omega C_2} + Z_L \right)} \quad (3.16)$$

$$A_{SP} = \frac{v_{out}}{v_{in}} = \frac{-j\omega M Z_L}{Z_{Link} \left((j\omega L_2 + R_2)(j\omega C_2 Z_L + 1) + Z_L \right)} \quad (3.17)$$

$$A_{PS} = \frac{v_{out}}{v_{in}} = \frac{-j\omega M Z_L Z_{Link}}{(j\omega L_1 + R_1 + Z_{refl}) \left(j\omega L_2 + R_2 + \frac{1}{j\omega C_2} + Z_L \right)} \quad (3.18)$$

$$A_{PP} = \frac{v_{out}}{v_{in}} = \frac{-j\omega M Z_L Z_{Link}}{(j\omega L_1 + R_1 + Z_{refl}) \left((j\omega L_2 + R_2)(j\omega C_2 Z_L + 1) + Z_L \right)} \quad (3.19)$$

Table 3.1. Link impedances for different link topologies [27]

Topology	Link impedance, Z_{Link}
SS	$j\omega L_1 + R_1 + \frac{1}{j\omega C_1} + \frac{(\omega M)^2}{j\omega L_2 + R_2 + \frac{1}{j\omega C_2} + Z_L}$
SP	$j\omega L_1 + R_1 + \frac{1}{j\omega C_1} + \frac{(\omega M)^2}{j\omega L_2 + R_2 + \frac{Z_L}{1 + j\omega C_2 Z_L}}$
PS	$\left(j\omega C_1 + \frac{1}{j\omega L_1 + R_1 + \frac{(\omega M)^2}{j\omega L_2 + R_2 + \frac{1}{j\omega C_2} + Z_L}} \right)^{-1}$
PP	$\left(j\omega C_1 + \frac{1}{j\omega L_1 + R_1 + \frac{(\omega M)^2}{j\omega L_2 + R_2 + \frac{Z_L}{1 + j\omega C_2 Z_L}}} \right)^{-1}$

The output power P_{out} is defined as follows:

$$P_{out} = \frac{|v_{out}|^2 Re\{Z_L\}}{|Z_L|^2} \quad (3.20)$$

The total link efficiency η_{Link} can be calculated as the product of two efficiencies; the efficiency from power source to Z_{refl} , which is referred to as η_1 and the second one is η_2 , which is the efficiency from receiver to Z_L . The efficiencies η_1 , η_2 , η_{Link} are defined by [27]

$$\eta_1 = \frac{P_{Z_{refl}}}{P_{in}} = \frac{|i_1|^2 Re\{Z_{refl}\}}{|i_{in}|^2 Re\{Z_{Link}\}} = \frac{|i_1|^2 Re\{Z_{refl}\} |Z_{Link}|^2}{|v_{in}|^2 Re\{Z_{Link}\}} \quad (3.21)$$

$$\eta_2 = \frac{P_{out}}{P_{Z_{refl}}} = \frac{|v_{out}|^2 Re\{Z_L\}}{|i_1|^2 Re\{Z_{refl}\} |Z_L|^2} \quad (3.22)$$

$$\eta_{Link} = \eta_1 \eta_2 = \frac{P_{Z_{refl}} P_{out}}{P_{in} P_{Z_{refl}}} = \frac{P_{out}}{P_{in}} \quad (3.23)$$

The coupling coefficient K between two spirals coils shown in Figure 3.4 can be given by

$$K = \left[\frac{1}{\left[1 + 2^{\frac{2}{3}} \left(\frac{d}{\sqrt{r_t * r_r}} \right)^2 \right]^{\frac{2}{3}}} \right] \cos \varphi \quad (3.24)$$

Where, r_t and r_r are the radii of transmitting and receiving coils, respectively. d is the direct distance between the centers of the two coils and φ is the misalignment angle.

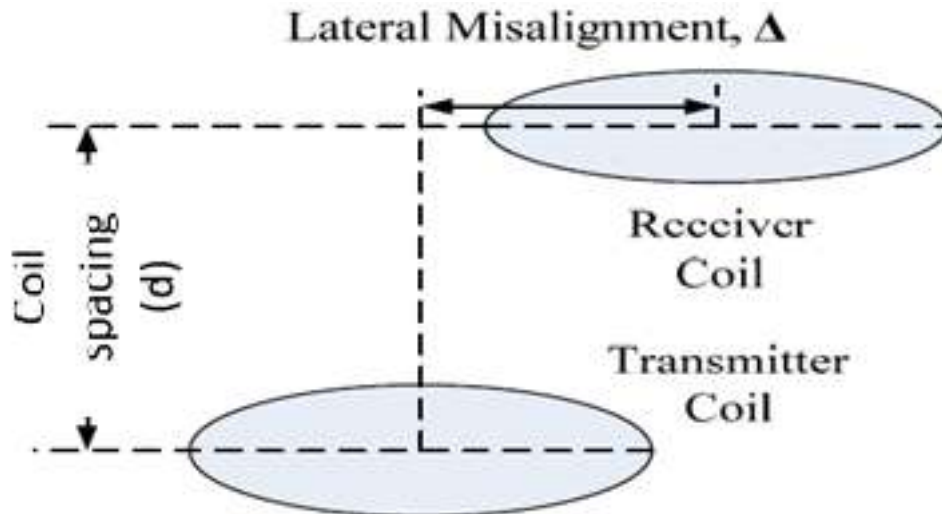


Figure.3.4. Variation effects of lateral misalignment (φ) between the transmitting and the receiving coils.

3.4. Proposed WPT System for Skin Implantable Biosensors

The circuit is designed on PSpice Orcad16.6. Figure 3.5 shows the circuit design of the first proposed wireless powering system for implantable biosensors in human skin.

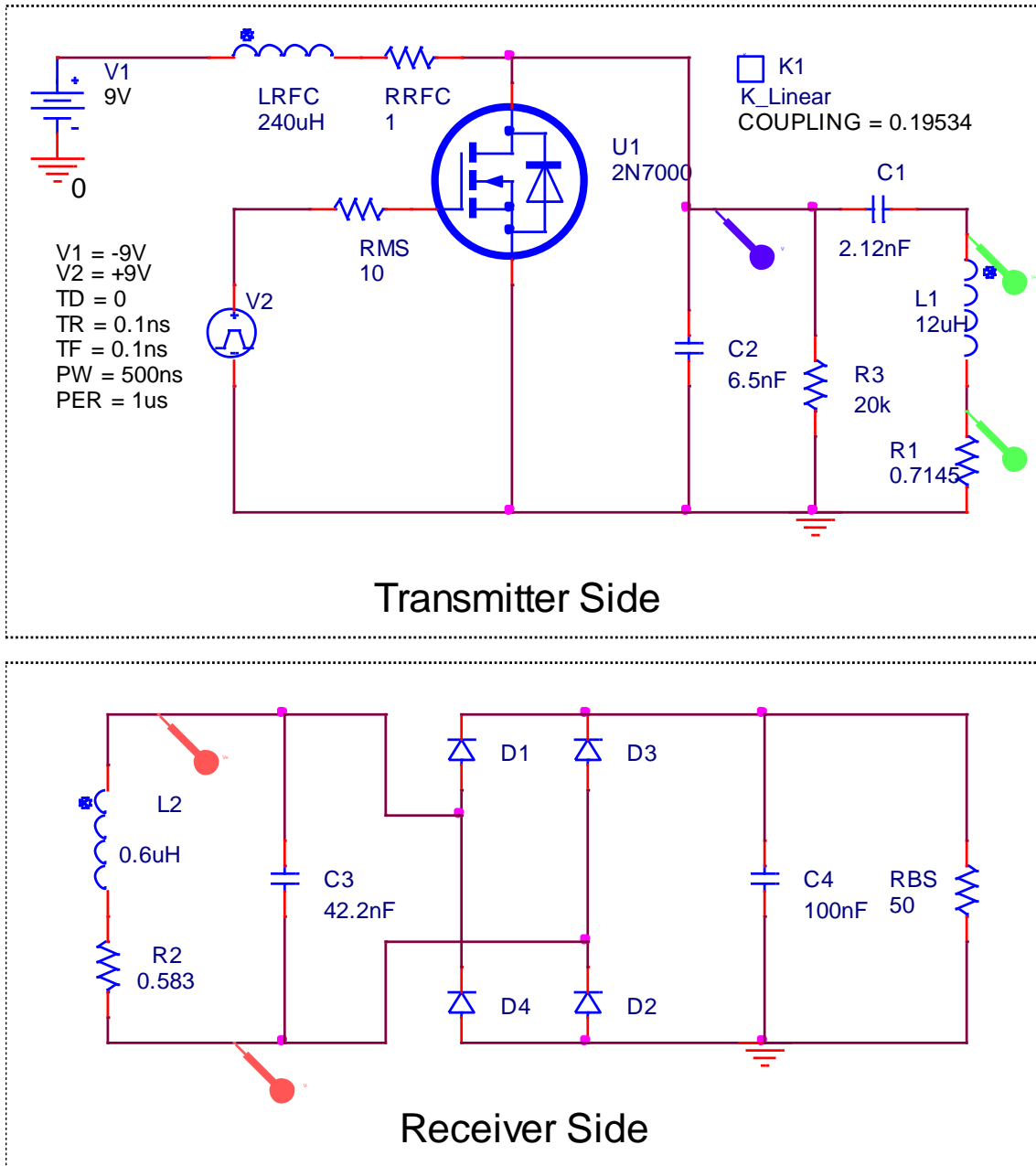


Figure 3.5. The Proposed Wireless Powering System for Skin Implantable Biosensors

The distance between transmitting and receiving coils is 1cm or less. The transmitting circuit is built of a class-E power amplifier loaded by a parallel combination of C_2 and the series resonator formed by L_1 and C_1 . The amplifier is designed to operate at a frequency f of 1MHz. The coil L_1 represents the transmitting coil, while the coil L_2

represents the receiving coil. According to class-E design methodology, the series combination L_1C_1 resonates at a frequency slightly less than f . whereas the parallel combination of C_2 and L_1C_1 resonates at f in order to minimize the operating current of the MOSFET. The receiving coil is designed as a planar spiral coil specified by outer diameter $d_o=8\text{mm}$, inner diameter $d_i=3\text{mm}$, number of turns $N=10$, conductor diameter $w=0.2\text{mm}$, and spacing between conductors $s=0.05\text{mm}$. The coil conductor material is Platinum, which has an electrical conductivity σ of $9.43 \times 10^6 \text{ } \Omega/\text{m}$. The calculated inductance L_2 and resistance R_2 are $0.6\mu\text{H}$ and 0.583Ω , respectively. The transmitting coil is designed as a planar spiral coil, which is specified by outer diameter $d_o=20\text{mm}$, inner diameter $d_i=2\text{mm}$, number of turns $N=38$, conductor diameter $w=0.2\text{mm}$, and spacing between conductors $s=0.036842\text{mm}$. The coil conductor material is Copper, which has an electrical conductivity σ of $5.85 \times 10^7 \text{ } \Omega/\text{m}$. The calculated inductance L_1 and resistance R_1 are $12\mu\text{H}$ and 0.7145Ω , respectively. For a distance of 1cm between the aligned receiving and transmitting coils, the coupling coefficient K according to Equation (24) is calculated as 0.19534 .

3.5. The Proposed WPT System for deep Implantable Biosensors

Figure 3.5 shows the circuit design of the second proposed wireless powering system for deep implantable biosensors. In this case, the distance between transmitting and receiving coils is 30cm or less. Such kinds of systems are capable of energizing deep biosensors in human body in addition of their capabilities of charging batteries embedded for various stimulation purposes. In this system, a receiving coil similar to that specified for the first system is chosen. For delivering more power to the embedded biosensor, a transmitting coil of an outer diameter of 10cm and inner diameter of 2cm is chosen.

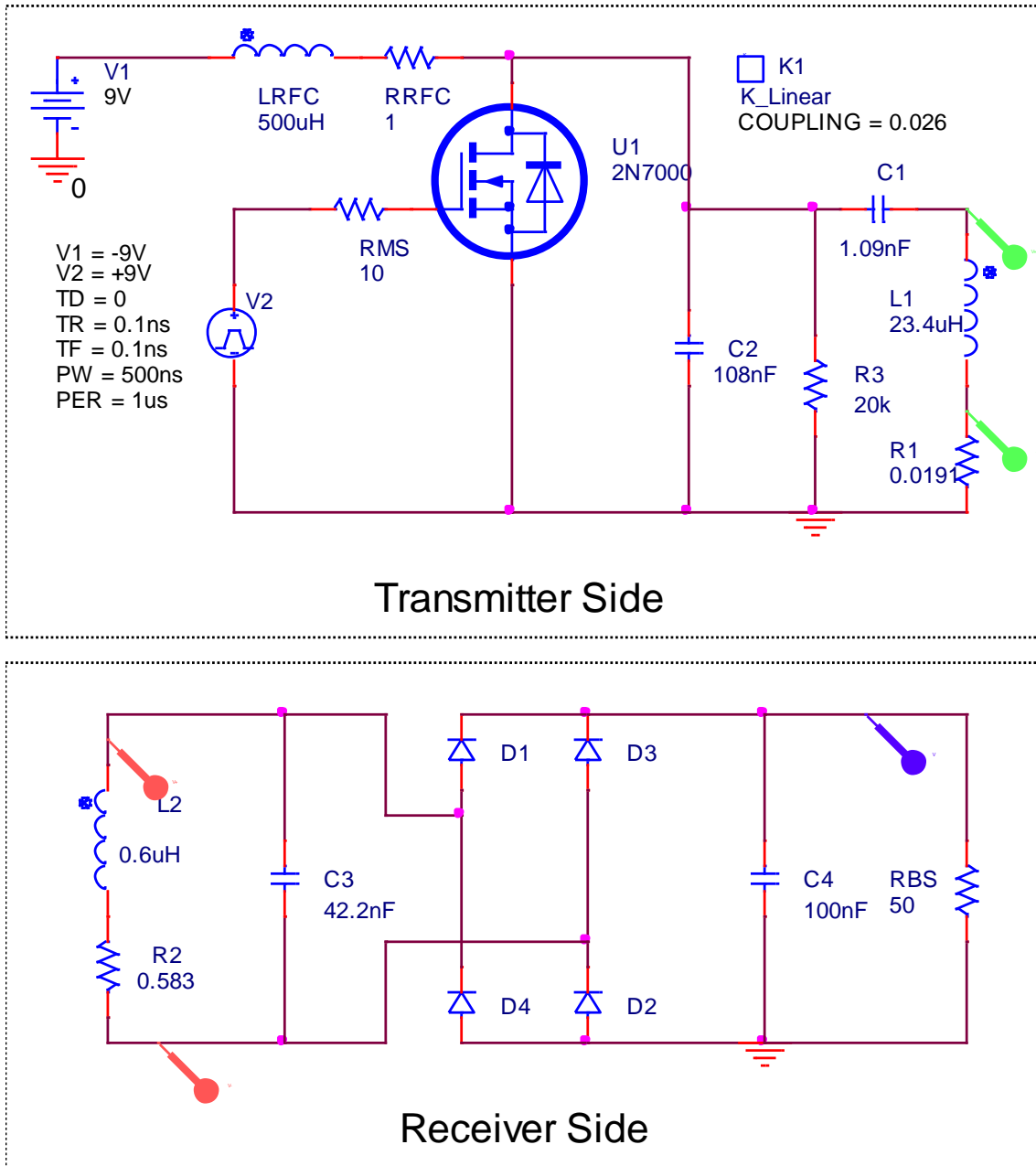


Figure 3.5. The Proposed Wireless Powering System for Skin Implantable Biosensors

The selected distance between transmitting and receiving coils is 30cm. The transmitting circuit is similar to that of the first system except the circuit parameter values. The amplifier is designed to operate at a frequency f of 1MHz. The transmitting coil is designed as a planar spiral coil specified by outer diameter $d_0=30$ cm, inner

diameter $d_i=2\text{cm}$, number of turns $N=14$, conductor diameter $w=4\text{mm}$, and spacing between conductors $s= 6\text{mm}$. The coil conductor material is Copper, which has an electrical conductivity σ of $5.85 \times 10^7 \text{ S/m}$. The calculated inductance L_I and resistance R_I are $23.3945\mu\text{H}$ and 0.0191Ω , respectively. For a distance of 30cm between the aligned receiving and transmitting coils, the coupling coefficient K according to Equation (24) is calculated as 0.026.

CHAPTER FOUR

RESULTS AND DISCUSSION

4.1. Introduction

The circuits of Figure 3.5 and Figure 3.6 were tests on PSpice for investigating their performance during energizing their corresponding biosensors. In this work, biosensors intended to be powered are replaced by certain resistors for simplicity.

4.2. Results of Powering Skin Implantable Biosensors

The circuit of Figure 3.5, which concerns the powering process of biosensors implanted directly in or under the human skin. The first test was carried out during wirelessly energizing a 50Ω biosensor. Figure 4.1 shows the DC supply voltage V_{DC} , the DC supply current I_{DC} and the output DC voltage or biosensor voltage V_{BS} . The figure shows that the biosensor voltage approached its steady state after $50\mu\text{s}$ with a DC power of $P_{BS} = (V_{BS})^2/50 = (6.5)^2/50 = 845\text{mW}$. The DC power drawn from the DC source is $P_{DC} = V_{DC}I_{DC} = 9 \times 0.65 = 5.85\text{W}$. Link efficiency is $(P_{BS}/P_{DC}) \times 100\% = 14.444\%$.

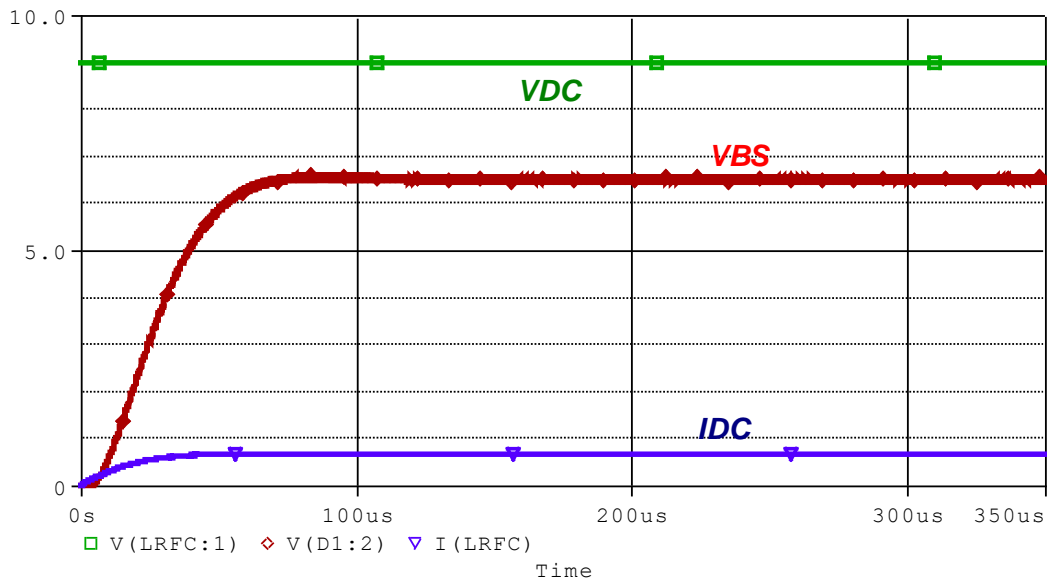


Figure 4.1. Powering of 50Ω skin implantable biosensor.

Figure 4.2 shows the transmitting coil voltage V_{L1} , the receiving coil voltage V_{L2} , and the biosensor voltage V_{BS} .

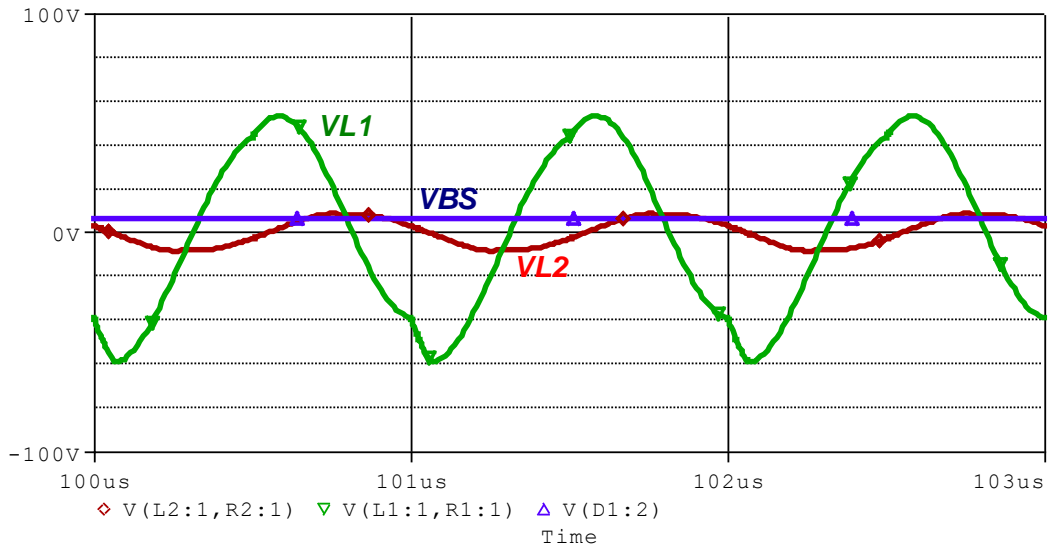


Figure 4.2. The transmitting coil voltage V_{L1} , the receiving coil voltage V_{L2} , and the biosensor voltage V_{BS} during powering a 50Ω biosensor.

The second was carried out during wireless powering of 100Ω biosensor. Figure 4.3 shows that the biosensor voltage reached its steady state within $50\mu\text{s}$ too with a DC power of $P_{BS} = (7.5)^2/100 = 562.5\text{mW}$.

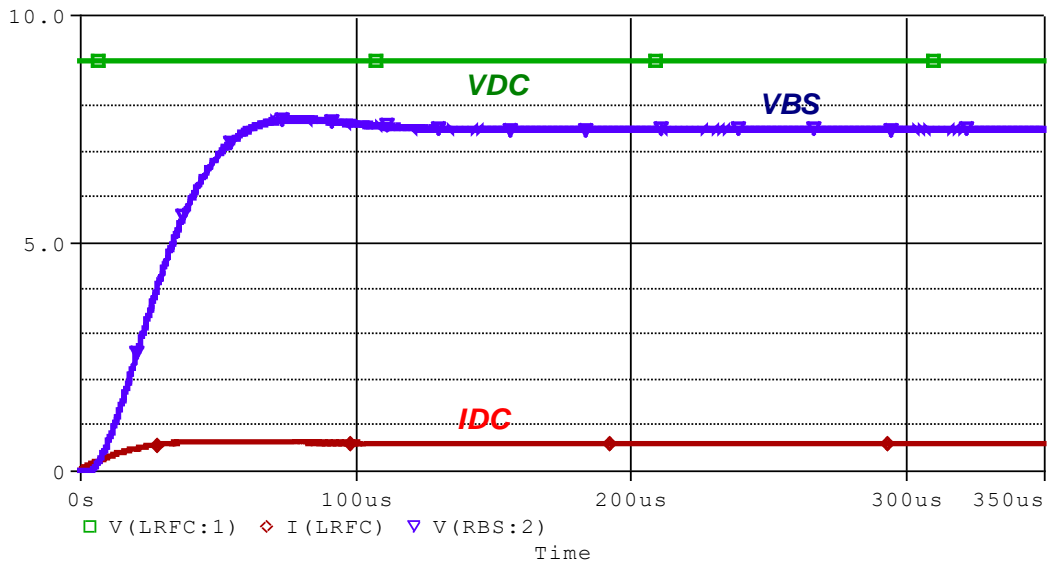


Figure 4.3. Powering of 100Ω skin implantable biosensor.

The DC power drawn from the DC source is $P_{DC} = 9 \times 0.6 = 5.4\text{W}$. Link efficiency is $(P_{BS}/P_{DC}) \times 100\% = 10.416\%$. Figure 4.4 shows the transmitting coil voltage V_{L1} , the receiving coil voltage V_{L2} , and the biosensor voltage V_{BS} .

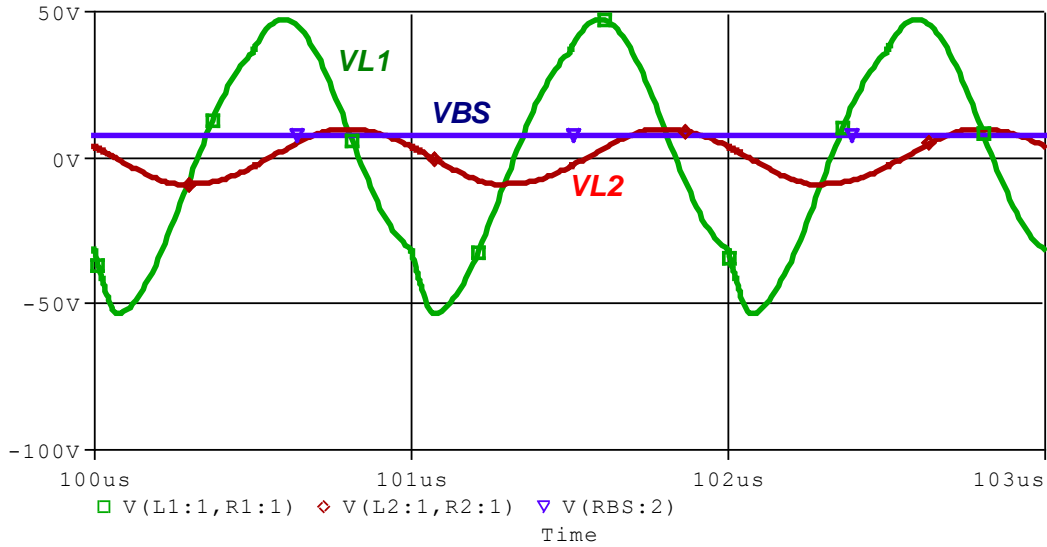


Figure 4.4. The transmitting coil voltage V_{L1} , the receiving coil voltage V_{L2} , and the biosensor voltage V_{BS} during powering a 100Ω biosensor.

The third test was carried out during powering a 200Ω biosensor. Figure 4.5 shows that the biosensor voltage of 8.1V with a DC power of $P_{BS} = (8.1)^2/200 = 328.05\text{mW}$. The DC power drawn from the DC source is $P_{DC} = 9 \times 0.56 = 5.04\text{W}$. Link efficiency is $(P_{BS}/P_{DC}) \times 100\% = 6.5\%$. It is obvious, that the efficiency decreases with the increase of biosensor impedance. Maximum efficiency occurs when the biosensor impedance made equal the output impedance of the inductive link.

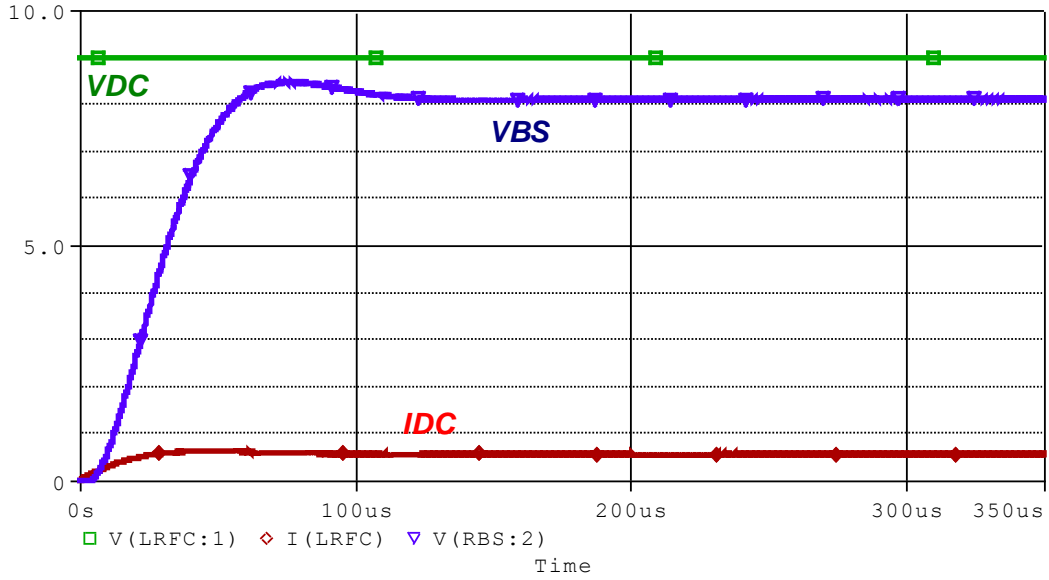


Figure 4.5. Powering of 200Ω skin implantable biosensor.

Figure 4.6 shows the transmitting coil voltage V_{L1} , the receiving coil voltage V_{L2} , and the biosensor voltage V_{BS} .

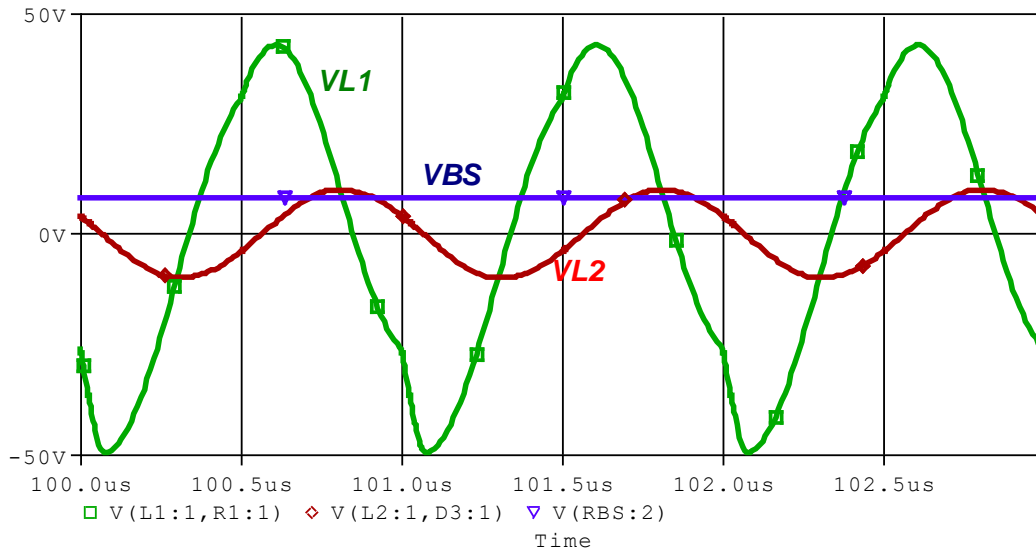


Figure 4.6. The transmitting coil voltage V_{L1} , the receiving coil voltage V_{L2} , and the biosensor voltage V_{BS} during powering a 200Ω biosensor.

4.3. Results of Powering Deeply embedded Biosensors

The circuit of Figure 3.6, which concerns the powering process of deeply embedded biosensors. Similar to what had been for skin embedded biosensors, the first test was carried out during energizing a 50Ω biosensor. Figure 4.7 shows the DC supply voltage V_{DC} , the DC supply current I_{DC} and the output DC voltage or biosensor voltage V_{BS} . The figure shows that the biosensor voltage approached its steady state after $250\mu s$ with a DC power of $P_{BS} = (V_{BS})^2/50 = (6.7)^2/50 = 897.8mW$. The DC power drawn from the DC source is $P_{DC} = V_{DC}I_{DC} = 9 \times 1.133 = 10.197W$. Link efficiency is $(P_{BS}/P_{DC}) \times 100\% = 8.8\%$.

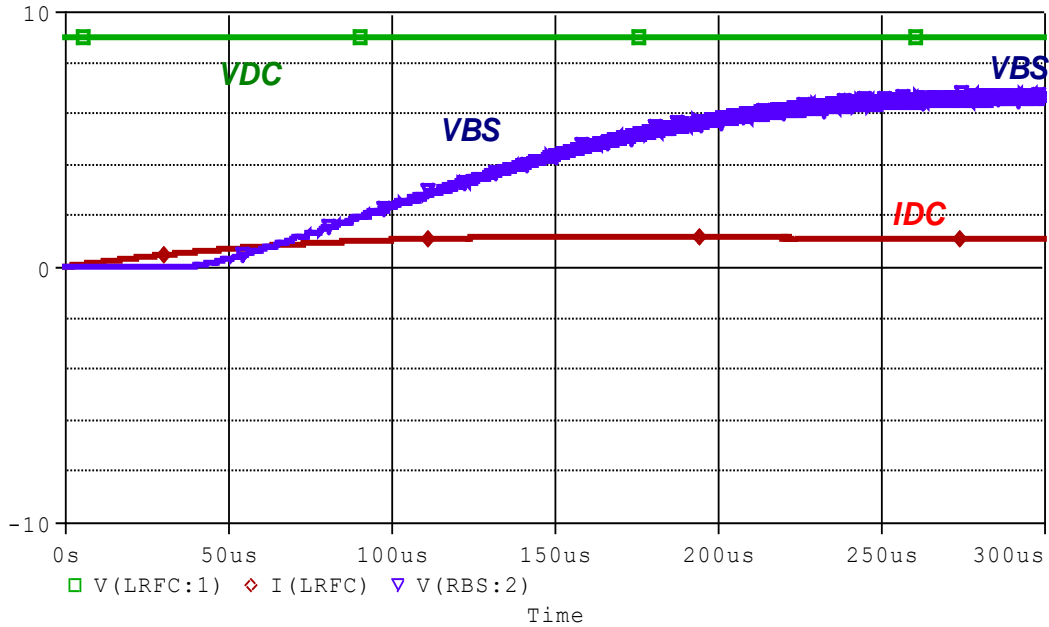
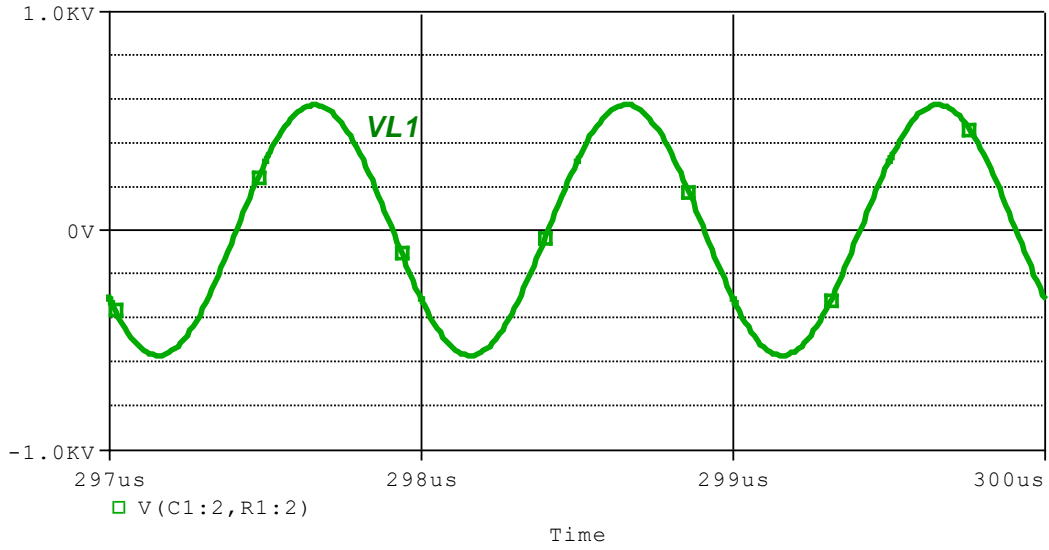
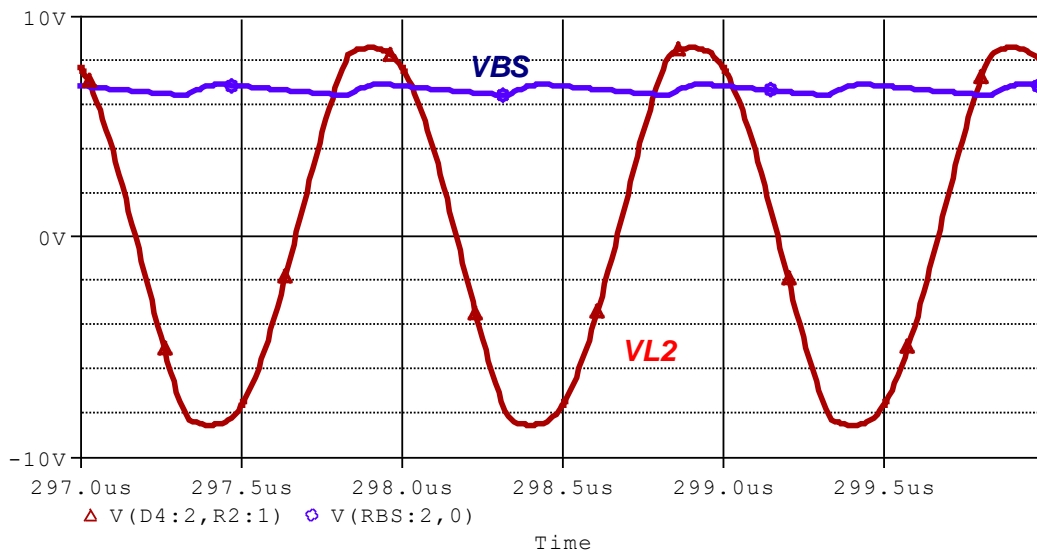


Figure 4.7. Powering of 50Ω deeply embedded biosensor.

Figure 4.8a shows the transmitting coil voltage V_{L1} , while Figure 8b shows the receiving coil voltage V_{L2} , and the biosensor voltage V_{BS} . The figure reveals very high voltage across the transmitting coil in comparison with voltage across the receiving coil.



(a)



(b)

Figure 4.8. The inductive link voltages during wireless powering of 50Ω deeply embedded biosensor, (a) the transmitting coil voltage V_{L1} and (b) the receiving coil voltage V_{L2} and the biosensor voltage V_{BS} .

The second test was carried after replacing the biosensor by a battery and a small series coil of $10\mu\text{H}$, which are located inside the human body at a depth of 30cm. Figure 9 shows the DC supply current and the embedded battery DC current. The wireless powering system had delivered a charging current I_{CG} of 200mA to battery even though the DC source current is about 1A.

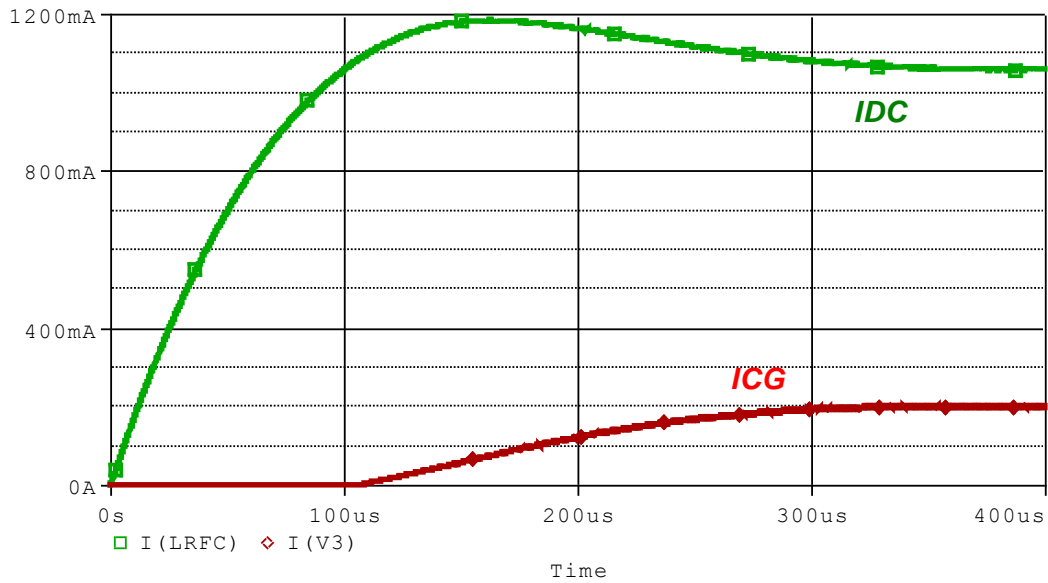


Figure 4.9. Charging an implantable 5V chargeable battery at a depth of 30cm inside the human body.

CHAPTER FIVE

CONCLUSION AND FUTURE WORK

5.1. Conclusion

In this work, the idea of wireless of energizing of biosensors has been verified using inductive coupling modality for both surface biosensors and deeply implanted ones. Even though, the efficiency of both system is small, but it offers the avoidance of surgical process during replacing the battery of the implanted sensor. In addition, wireless powering offers the feasibility of employing long lifetime biosensors.

5.2. Future Work

The future work concerning these wireless powering processes is dealt with possibility equipping the biosensors with electronic circuitries for exchanging data with certain servers.

REFERENCES

- [1] Rita Rebelo, Ana Isabel Barbosa, Vitor M. Correlo, Rui L. Reis, "An Outlook on Implantable Biosensors for Personalized Medicine," *Engineering*, Vol. 7, No. 12, pp. 1696-1699, 2021.
- [2] M. Haerinia, "A State of Art Review on Wireless Power Transmission Approaches for Implantable Medical Devices," *arXiv: Signal Processing*, p. 21, 2020.
- [3] Bhagwati Charan Patel, G R Sinha, and Naveen Goel, "Advances in Modern Sensors," *IOP Publishing, chapter one*, p. 22, 2020.
- [4] J. -D. Kim, C. Sun and I. -S. Suh, "A proposal on wireless power transfer for medical implantable applications based on reviews," *2014 IEEE Wireless Power Transfer Conference*, pp. 166-169, 2014.
- [5] Ghafar-Zadeh E. Wireless integrated biosensors for point-of-care diagnostic applications," *Sensors (Basel)*, 15(2), pp. 3236-3261, Feb 2015.
- [6] Janko Katic, "Efficient Energy Harvesting Interface for Implantable Biosensors," Licentiate Thesis, KTH Royal Institute of Technology Stockholm, Stockholm, Sweden, p. 90, 2015.
- [7] Fanpeng Kong, "Coil Misalignment Compensation Techniques for Wireless Power Transfer Links in Biomedical Implants," MSc Thesis, The State University of New Jersey, New Jersey, USA, p. 69, October, 2015.
- [8] E. G. Kilinc *et al.*, "A System for Wireless Power Transfer and Data Communication of Long-Term Bio-Monitoring," in *IEEE Sensors Journal*, vol. 15, no. 11, pp. 6559-6569, Nov. 2015.
- [9] Kyle A. Thackston, "Optimization of Wireless Power Networks for Biomedical Applications," MSc Thesis, Purdue University, West Lafayette, Indiana, USA, 2016.
- [10] Schormans M, Valente V, Demosthenous A. Frequency Splitting Analysis and Compensation Method for Inductive Wireless Powering of Implantable Biosensors. *Sensors (Basel)*. 16(8), p. 14, Aug 2016.

- [11] S. Peng, M. Liu, Z. Tang and C. Ma, "Optimal design of megahertz wireless power transfer systems for biomedical implants," *2017 IEEE 26th International Symposium on Industrial Electronics (ISIE)*, pp. 805-810, 2017.
- [12] Reem Shadid, "Wireless Power Transfer for Biomedical Applications," PhD Thesis, University of North Dakota, North Dakota, USA, p. 146, May 2018.
- [13] Max Grell, Can Dincer, Thao Le, Alberto Lauri, Estefania Nunez Bajo, Michael Kasimatis, Giandrin Barandun, Stefan A. Maier, Anthony E. G. Cass, and Firat Güder, "Autocatalytic Metallization of Fabrics Using Si Ink, for Biosensors, Batteries and Energy Harvesting," *Advanced Functional Materials*, 29(1), January 2019.
- [14] Hammad Saleem, Muhammad Awais, Siraj Din, Attequa, and Asma Mahar, "Wireless Power Transfer and Data Communication for Biomedical Application," *The 2019 International Conference on Artificial Life and Robotics (ICAROB2019)*, Jan. 10-13, B-Con Plaza, Beppu, Oita, Japan, pp. 707-711, 2019.
- [15] Sadeque Reza Khan, "Design, manufacture and performance characterization of wireless power transfer systems for biomedical devices," PhD Thesis, Heriot-Watt University, Edinburgh EH14 4AS, United Kingdom, p. 249, 2019.
- [16] Q. Xu, T. Wang, S. Mao, W. Jia, Z. Mao, and M. Sun, "Wireless Power Transfer for Miniature Implantable Biomedical Devices", in *Recent Wireless Power Transfer Technologies*. London, United Kingdom: IntechOpen, 2019.
- [17] Mustafa Adil Hussain and Sadik Kamel Gharghan and Haider Qasim Hamood, "Design and Implementation of Wireless Low-Power Transfer for Medical Implant Devices," *IOP Conference Series: Materials Science and Engineering*, 2020 IOP Conf. Ser.: Mater. Sci. Eng. 745 012087, p. 20, 2020.
- [18] Daniela Rodrigues 1 , Ana I. Barbosa 1,2, Rita Rebelo 1,2 , Il Keun Kwon 1, Rui L. Reis 1,2,3 and Vitor M. Correlo, "Skin-Integrated Wearable Systems and Implantable Biosensors: A Comprehensive Review," *Biosensors*, 10(79), p.28, 2020.
- [19] Akram, M.A.; Yang, K.-W.; Ha, S. Duty-Cycled Wireless Power Transmission for Millimeter-Sized Biomedical Implants. *Electronics*, 9, p. 15, 2020.

- [20] D.B.Ahire¹ and Vitthal J.Gond, "Design and Simulation of Wireless Power Transfer System for Biomedical Implant." *International Journal of Advanced Science and Technology*, Vol. 29, No. 9s, pp. 7496-7514, 2020.
- [21] Khan SR, Pavuluri SK, Cummins G, Desmulliez MPY. Wireless Power Transfer Techniques for Implantable Medical Devices: A Review. *Sensors*, 20(12), p. 58, 2020.
- [22] Mohammad Haerinia, and Reem Shadid, "Wireless Power Transfer approaches for Medical Implants: A Review," *Signals*, 1, pp. 209-229, 2020.
- [23] Yu Song, Jihong Min, You Yu, Haobin Wang, Yiran Yang, Haixia Zhang, and Wei Gao, "Wireless battery-free wearable sweat sensor powered by human motion," *Sci. Adv.* 2020; 6, p. 10, Sep. 2020.
- [24] A. Iqbal, M. Al-Hasan, I. B. Mabrouk, A. Basir, M. Nedil and H. Yoo, "Biotelemetry and Wireless Powering of Biomedical Implants Using a Rectifier Integrated Self-Diplexing Implantable Antenna," in *IEEE Transactions on Microwave Theory and Techniques*, vol. 69, no. 7, pp. 3438-3451, July 2021.
- [25] Muayad Kod, Jiafeng Zhou, Yi Huang, Muaad Hussein, Abed P. Sohrab, and Chaoyun Song, "An Approach to Improve the Misalignment and Wireless Power Transfer into Biomedical Implants Using Meandered Wearable Loop Antenna," *Wireless Power Transfer*, Vol. 2021, p. 12, 2021.
- [26] Ramesh K. Pokharel, Adel Barakat, Shimaa Alshhawy, Kuniaki Yoshitomi and Costas Sarris, "Wireless power transfer system rigid to tissue characteristics using metamaterial inspired geometry for biomedical implant applications," *Sci Rep* 11, 5868, p. 10, 2021.
- [27] M. Schormans, V. Valente, and A. Demosthenous, "Practical Inductive Link Design for Biomedical Wireless Power Transfer: A Tutorial," *IEEE Transactions on Biomedical Circuits and Systems*, vol. 12, no. 5, pp. 1112 - 1130, 2018.
- [28] R. Ludwig and P. Bretchko, "RF Circuit Design: Theory & Applications," Prentice Hall, Upper Saddle River, New Jersey, USA, 2000.

- [29] X. Mou and H. Sun, "Wireless Power Transfer: Survey and Roadmap," *2015 IEEE 81st Vehicular Technology Conference (VTC Spring)*, 2015, pp. 1-5, doi: 10.1109/VTCSpring.2015.7146165.